LETTER

doi:10.1038/nature25744

Mechanical regulation of stem-cell differentiation by the stretch-activated Piezo channel

Li He[1], Guangwei Si[2], Jiuhong Huang[3], Aravinthan D. T. Samuel[2] & Norbert Perrimon[1,4]

Somatic stem cells constantly adjust their self-renewal and lineage commitment by integrating various environmental cues to maintain tissue homeostasis. Although numerous chemical and biological signals have been identified that regulate stem-cell behaviour, whether stem cells can directly sense mechanical signals *in vivo* remains unclear[1]. Here we show that mechanical stress regulates stem-cell differentiation in the adult *Drosophila* midgut through the stretch-activated ion channel Piezo. We find that *Piezo* is specifically expressed in previously unidentified enteroendocrine precursor cells, which have reduced proliferation ability and are destined to become enteroendocrine cells. Loss of *Piezo* activity reduces the generation of enteroendocrine cells in the adult midgut. In addition, ectopic expression of *Piezo* in all stem cells triggers both cell proliferation and enteroendocrine cell differentiation. Both the *Piezo* mutant and overexpression phenotypes can be rescued by manipulation of cytosolic Ca^{2+} levels, and increases in cytosolic Ca^{2+} resemble the Piezo overexpression phenotype, suggesting that Piezo functions through Ca^{2+} signalling. Further studies suggest that Ca^{2+} signalling promotes stem-cell proliferation and differentiation through separate pathways. Finally, *Piezo* is required for both mechanical activation of stem cells in a gut expansion assay and the increase of cytosolic Ca^{2+} in response to direct mechanical stimulus in a gut compression assay. Thus, our study demonstrates the existence of a specific group of stem cells in the fly midgut that can directly sense mechanical signals through Piezo.

Drosophila midgut stem cells have emerged as an attractive *in vivo* model for understanding adult stem-cell behaviours[2–4]. Like their mammalian counterparts, fly intestinal stem cells (ISCs) produce two major classes of cells that compose the adult intestinal epithelium: absorptive enterocytes and secretory enteroendocrine cells (EEs)[4]. Many extrinsic signals, including chemicals, nutrition, pathogens and cytokines, have been shown to regulate ISC proliferation and differentiation[4,5]. However, whether midgut stem cells can sense biomechanical signal remains unknown.

From a screen of GAL4 lines with expression in *Drosophila* midgut, we identified *PiezoP-GAL4* (BL59266, Bloomington *Drosophila* Stock Center)[6], a GAL4 transgene under control of a cloned enhancer/promoter region of *Piezo*, which was expressed in a subpopulation of Escargot (Esg)-positive stem cells in the adult fly midgut (Extended Data Fig. 1a). Piezo is a cation ion channel that directly senses mechanical tension in lipid bilayers[7]. It was initially identified in mammalian cells as a touching sensor[8], and was further found to be responsible for mechanoreception in different cell types[9]. The *Drosophila* genome encodes a single *Piezo* homologue, which has been characterized previously as a receptor for mechanotransduction in sensory neurons[6,10].

To represent the expression pattern of *Piezo* accurately, we directly knocked-in the GAL4 transgene into the *Piezo* locus after the first start codon through homologous recombination (referred to as *Piezo-GAL4* hereafter; Extended Data Fig. 1b). The expression of red fluorescent protein (RFP) driven by *Piezo-GAL4* showed a pattern similar to BL59266 in Esg^+ cells, but was also detected in some enterocytes located in the cardia and copper and iron regions (Fig. 1a, Extended Data Fig. 1c–f, h), which is consistent with published *Piezo* mRNA profiles along the midgut[11] (Extended Data Fig. 1g). Because Esg is expressed in both ISCs and enteroblasts (progeny of ISCs that are destined to become enterocytes), we used the ISC-specific marker *Delta-lacZ* and the enteroblast marker *Su(H)Gbe-lacZ* to identify $Piezo^+$ cells precisely. Notably, *Piezo* is expressed in a subpopulation (approximately 40%) of Delta-positive (Dl^+) cells, and is absent from enteroblasts (Fig. 1a, Extended Data Fig. 1i). We also noticed that almost all 'newborn' EEs (positive for both Esg and the EE-specific marker Prospero) are also $Piezo^+$, suggesting that $Piezo^+$ cells may represent enteroendocrine cell precursors (Fig. 1c, Extended Data Fig. 1k, l). Indeed, G-TRACE[12]-labelled progenies of $Piezo^+$ cells are primarily EEs (approximately 90%), rather than 11% EEs from Dl^+ ISCs, and 99% enterocytes from $Su(H)Gbe^+$ enteroblasts (Fig. 1d, e, Extended Data Fig. 1m–o). In addition, damage caused by bleomycin[13] or inhibition of Notch by the γ-secretase inhibitor DAPT[14] promotes the generation of both EEs and $Piezo^+$ cells (Fig. 1f, Extended Data Fig. 2a). Finally, ablation of $Piezo^+$ cells using the pro-apoptotic protein Reaper (Rpr) notably reduced not only the number of $Piezo^+$ cells but also enteroendocrine cell numbers after 4 weeks (Fig. 1g, h), and both cell types are recovered after one week of suppression of Rpr expression (Fig. 1g, h), suggesting that $Piezo^+$ cells are an important source of enteroendocrine cell generation. We further investigated whether $Piezo^+$ cells are self-regenerative or primarily derived from ISCs. First, mitotic $Piezo^+$ cells (marked by anti-phospho-histone3 (pH3) staining) represent only a small portion (~10%) of the total mitotic cells (Fig. 1i, Extended Data Fig. 2c–f), suggesting that $Piezo^+$ cells have reduced proliferation abilities compared to $Piezo^-$ stem cells. Bleomycin damage promotes the mitosis of both $Piezo^+$ and $Piezo^-$ cells without increasing the percentage of $Piezo^+$ mitotic cells, suggesting that an intrinsic mechanism limits the proliferation ability of $Piezo^+$ cells (Extended Data Fig. 2d, e). Finally, random green fluorescent protein (GFP)-marked clones generated from ISCs contain $Piezo^+$ cells, supporting the hypothesis that $Piezo^+$ cells are generated from ISCs (Extended Data Fig. 2g).

Taken together, our data suggest that previously considered Dl^+ ISCs are heterogeneous and composed of approximately 60% mitotic active multipotent ISCs ($Piezo^-$) and 40% less-mitotic unipotent $Piezo^+$ cells that mainly generate enteroendocrine cells. To avoid confusion with true ISCs (mitotic active and multipotent) and enteroblasts (occasionally referred to as Notch-active enterocyte progenitors), we refer to these $Piezo^+$ population as enteroendocrine precursors.

To investigate the function of Piezo, we analysed the phenotype of $Piezo^{KO}$, a null allele with a complete deletion of the *Piezo* coding sequence[6]. Midguts from $Piezo^{KO}$ homozygous flies showed no obvious phenotypes as compared to control flies during the early developmental and young adult stages, although Piezo is expressed in some stem cells during the larval and pupal stages (Extended Data Fig. 3). In wild-type

[1]Department of Genetics, Harvard Medical School, Boston, Massachusetts 02115, USA. [2]Department of Physics, Center for Brain Science, Harvard University, Cambridge, Massachusetts 02142, USA. [3]School of Life Science and Technology, Tongji University, Shanghai 200092, China. [4]Howard Hughes Medical Institute, Boston, Massachusetts 02115, USA.

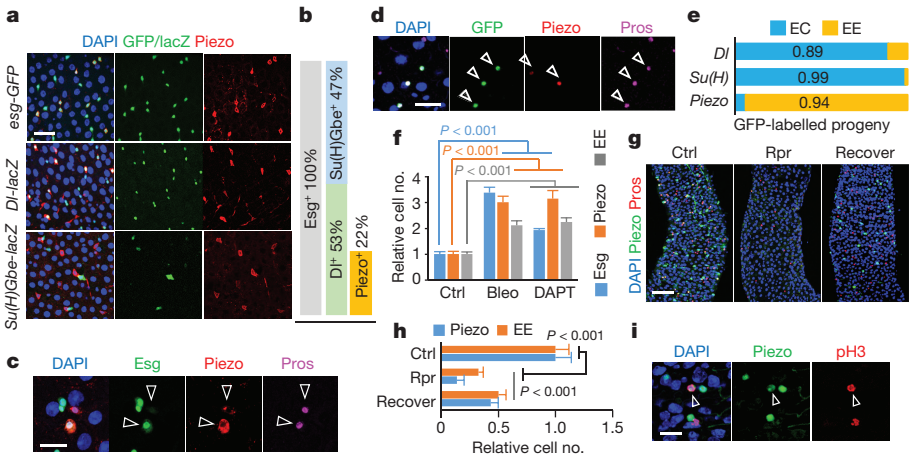

Figure 1 | Piezo$^+$ cells are EE precursors in the fly midgut. a, Piezo$^+$ cells (RFP$^+$, red) are Esg$^+$ (GFP, green) and Dl$^+$ (LacZ, green), but Su(H) Gbe$^-$ (LacZ, green). **b**, Percentage of Piezo$^+$ cells in Esg$^+$ cells. For Dl$^+$: $n = 238$ (Dl$^+$), $n = 457$ (Esg$^+$). For Piezo$^+$: $n = 151$ (Piezo$^+$), $n = 682$ (Esg$^+$). **c**, Newborn EEs (arrowheads) are Piezo$^+$ (mCherry$^+$, red; measured by *Piezo-GAL4*, *UAS-mCherry*) and Esg$^+$ (GFP$^+$, green; labelled by *esg-GFP*). **d**, Piezo$^+$ cells (RFP$^+$, red) generate GFP$^+$ EEs (arrowheads). **e**, Statistics of GFP$^+$ enterocytes (ECs) and EEs using *GAL4* lines *Piezo-GAL4*, *Su(H)Gbe-GAL4* and *Dl-GAL4*. Number of cells analysed: $n = 561$ (*Dl*), $n = 432$ (*Su(H)Gbe*), $n = 90$ (*Piezo*). **f**, Treatment with bleomycin (bleo) and DAPT increases the number of Esg$^+$, Piezo$^+$ and EE cells. Areas quantified: $n = 23$ (control; ctrl), $n = 21$ (bleo), $n = 32$ (DAPT). **g**, **h**, Elimination of Piezo$^+$ cells by conditional expression of Rpr. Areas quantified: $n = 27$ (ctrl), $n = 29$ (Rpr), $n = 27$ (recover). **i**, pH3 staining (red) of mitotic enteroendocrine precursors (arrowheads). Data are mean and s.e.m. *P* values are from a two-tailed *t*-test. Scale bars, 20 μm (**a**), 10 μm (**c**, **d**, **i**) and 50 μm (**g**).

flies, the number of Esg$^+$ cells and EEs increases as the flies age[15]. However, in *Piezo^{KO}* mutants, the number of enteroendocrine cells, but not Esg$^+$ cells, does not increase (Fig. 2a, b), suggesting that the generation of EEs after adulthood is affected. Furthermore, *Piezo*-mutant clones generate 80% fewer EEs than controls, and this can be rescued by expressing GFP-tagged full-length Piezo (Fig. 2c, d). These data suggest that the reduced generation of EEs is an autonomous defect.

Previous studies have shown that *Piezo* functions through increases in cytosolic Ca^{2+} concentrations[16–19]. Consistently, knocking down *Stromal interaction molecule* (*Stim*), previously used as an effective target to decrease cytosolic Ca^{2+} levels[20], also led to the production of fewer EEs (Fig. 2c, d). Furthermore, increasing cytosolic Ca^{2+} by knocking down *plasma membrane calcium ATPase* (*PMCA*) or *Sarco/endoplasmic reticulum calcium ATPase* (*SERCA*) rescued and even reversed the reduction of EEs in the *Piezo* mutant (Fig. 2c, d).

Overexpression of *Piezo* in Esg$^+$ cells caused an increase in both Esg$^+$ cells and EEs, and this phenocopied the increase of Ca^{2+} achieved by *SERCA* reduction, overexpression of *inositol-1,4,5-trisphosphate receptor* (*InsP3R*, also known as *Itp-r83A*), *Stim* and *Orai* (*olf186-F*), and *PMCA* knockdown (Fig. 2e, Extended Data Figs 4a–c, 5). Calcium imaging shows that cytosolic Ca^{2+} is significantly increased by *Piezo* overexpression in the stem cells (Extended Data Fig. 6a–d, Supplementary Videos 1, 2). The *Piezo*-overexpression phenotype is suppressed by reducing cytosolic Ca^{2+} using RNA interference (RNAi) that targets either *Stim* or *InsP3R* (Fig. 2e, Extended Data Fig. 4a–c). Finally, damage caused by bleomycin triggers an upregulation of Ca^{2+} and an increase in the number of Esg$^+$ and EE cells in both wild-type and *Piezo^{KO}* midguts, supporting the idea that Ca^{2+} is the downstream effector of Piezo (Extended Data Figs 5d, e, 6e–h).

Inhibition of Notch signalling has been shown to promote both ISCs renewal and EE differentiation[14,21], even in EE progenitors that already

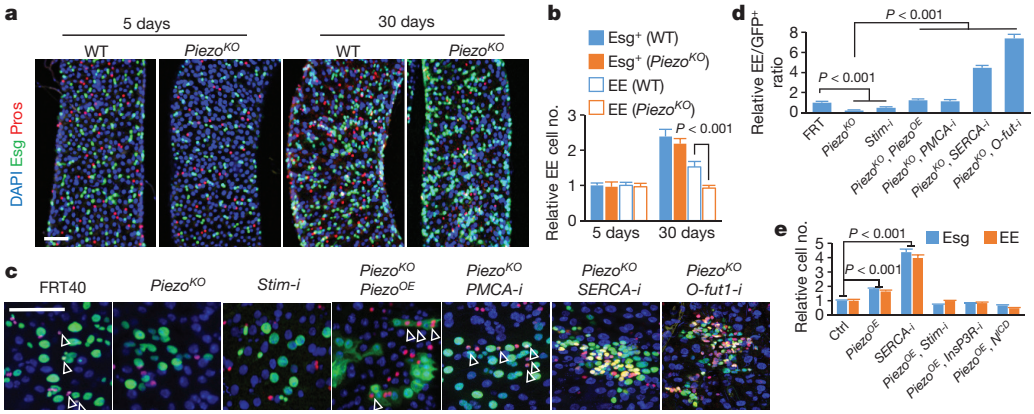

Figure 2 | Piezo regulates EE differentiation through cytosolic Ca^{2+}. a, **b**, Midgut of flies homozygous for the null mutant *Piezo^{KO}* shows reduced EE generation 30 days after eclosion. Areas quantified: $n = 32$ (wild type (WT) 5 days), $n = 32$ (WT 30 days), $n = 35$ (*Piezo^{KO}* 5 days), $n = 32$ (*Piezo^{KO}* 30 days). **c**, **d**, MARCM clones of cells with indicated genotypes (arrowheads indicate GFP$^+$ EEs). The ratio of EEs in the clone (normalized to control) is quantified. The '*-i*' suffix denotes RNAi. Number of clones quantified: $n = 32$ (*FRT*), $n = 35$ (*Piezo^{KO}*), $n = 26$ (*Stim-i*), $n = 28$ (*Piezo^{KO}*, *Piezo^{OE}*), $n = 31$ (*Piezo^{KO}*, *PMCA-i*), $n = 35$ (*Piezo^{KO}*, *SERCA-i*), $n = 28$ (*Piezo^{KO}*, *O-fut1-i*). **e**, Esg$^+$ and EE cell numbers were quantified in the indicated midgut-expressing genes using *esg-GAL4*. Number of areas quantified: $n = 22$ (ctrl), $n = 28$ (*Piezo^{OE}*), $n = 23$ (*SERCA-i*), $n = 21$ (*Piezo^{OE}*, *Stim-i*), $n = 24$ (*Piezo^{OE}*, *InsP3R-i*), $n = 26$ (*Piezo^{OE}*, *N^{ICD}*). Data are mean and s.e.m. *P* values are from a two-tailed Student's *t*-test. Scale bars, 50 μm (**a**) and 25 μm (**c**).

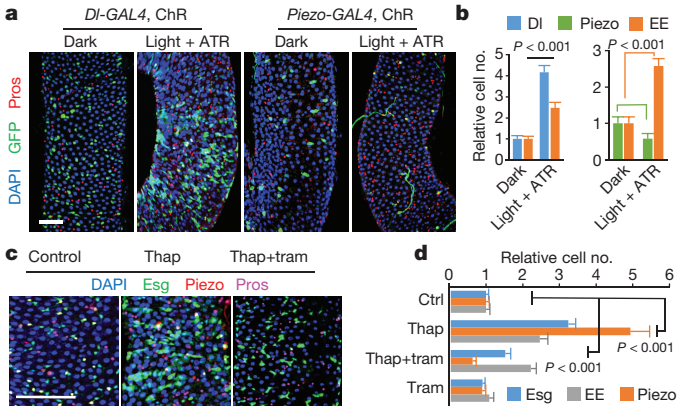

Figure 3 | Cytosolic Ca^{2+} triggers cell proliferation and EE differentiation through different mechanisms. **a**, **b**, Increase in cytosolic Ca^{2+} by channelrhodopsin (ChR) in Dl^+ and $Piezo^+$ enteroendocrine precursors. Dl^+, $Piezo^+$ and EE cell numbers are quantified (**b**). Number of areas quantified: $n = 28$ (dark, *Dl-GAL4*), $n = 30$ (light + ATR, *Dl-GAL4*), $n = 30$ (dark, *Piezo-GAL4*), $n = 31$ (light + ATR, *Piezo-GAL4*). **c**, **d**, Midguts of flies treated with thapsigargin (thap) and trametinib (tram). Number of areas quantified: $n = 29$ (ctrl), $n = 31$ (thap), $n = 32$ (thap + tram), $n = 29$ (tram). Data are mean and s.e.m. *P* values are from a two-tailed *t*-test. Scale bars, 50 μm.

have low Notch activity[22]. In addition, increases in cytosolic Ca^{2+} have been found to inhibit Notch activity in both cultured mammalian cells and flies[23,24]. We therefore tested whether Piezo functions through Notch inhibition by increasing cytosolic Ca^{2+}. Indeed, blocking Notch activation by knocking down the Notch-processing enzyme *O*-fucosyltransferase (encoded by *O-fut1*) reverses the Piezo-knockout phenotype (Fig. 2c, d, Extended Data Fig. 4h), and increasing Notch activity by expression of the Notch intracellular domain (N^{ICD}) blocks the phenotypes of both *Piezo* overexpression and *SERCA* knockdown (Fig. 2e, Extended Data Fig. 4a–g). Furthermore, overexpressing *Piezo* in Esg^+ cells produced more Dl^+ stem cells, consistent with a reduction in Notch activity (Extended Data Fig. 6i, j). Finally, neither *Piezo* overexpression nor *SERCA* knockdown had any effect in enteroblast cells (in which Notch has already been activated), suggesting that Notch signalling is the primary target (Extended Data Fig. 6k, l). Taken together, our data suggest that *Piezo* promotes EE differentiation by increasing cytosolic Ca^{2+} and inhibition of Notch.

To investigate the function of Ca^{2+} further, we used channelrhodopsin (ChR) to increase cytosolic Ca^{2+} levels optogenetically. Activation of ChR in Dl^+ cells promotes both ISC proliferation and EE production, resembling the *Piezo*-overexpression phenotype (Fig. 3a, b, Extended Data Fig. 7a–d). This ChR-induced phenotype is blocked by knockdown of both *Stim* and *InsP3R*, suggesting that the effect is Ca^{2+} dependent (Extended Data Fig. 7e, f). In addition, activation of ChR in $Piezo^+$ enteroendocrine precursors significantly increased the number of EE cells at the expense of precursor cells, suggesting an increase in the differentiation of enteroendocrine precursor to EEs (Fig. 3a, b). A recent study showed that Piezo activation promotes cell proliferation through Ca^{2+}-induced phosphorylation of ERK[19]. Consistently, overexpression of *Piezo* in Esg^+ cells increases phospho-ERK staining (Extended Data Fig. 7g). However, reducing ERK signalling through *Ras* knockdown or blocking cell proliferation by *yorkie* (*yki*) RNAi only affects cell proliferation, and not EE differentiation, in *Piezo*-overexpressing cells (Extended Data Fig. 7h–k), suggesting that Piezo promotes EE differentiation independently of proliferation. Consistently, increasing cytosolic Ca^{2+} using the SERCA inhibitor thapsigargin significantly increased stem-cell proliferation and EE generation (Fig. 3c, d). Further blocking mitosis using the MEK inhibitor trametinib only reduced thapsigargin-trigged proliferation, but not the increase in EE differentiation (Fig. 3c, d, Extended Data Fig. 7l–n). Ca^{2+} imaging showed that Ca^{2+} is increased in stem cells treated by thapsigargin, which is not blocked by trametinib (Extended Data Fig. 7o–q, Supplementary Video 3). Taken together, these data suggest that increases in cytosolic Ca^{2+} promote cell proliferation (through ERK phosphorylation) and cell differentiation (though Notch inhibition) in a cell-context-dependent manner.

To test whether mechanical challenges from food digestion can activate Piezo, we increased the mechanical load in the gastrointestinal

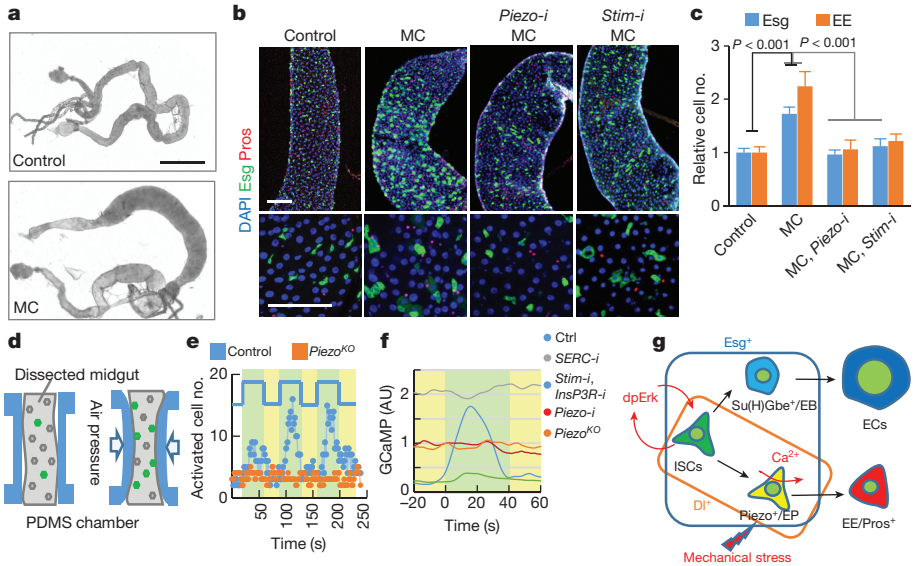

Figure 4 | Mechanical stress increases cytosolic Ca^{2+} through Piezo. **a**, Midgut of fly fed on food containing methylcellulose (MC). **b**, **c**, Methylcellulose feeding increases Esg^+ (GFP^+, green) and EE cell numbers in the midguts, which is blocked by *Piezo-i* and *Stim-i*. Number of areas quantified: $n = 25$ (ctrl), $n = 23$ (MC), $n = 20$ (MC + *Piezo-i*), $n = 25$ (MC + *Stim-i*). **d**, An illustrated microfluidic channel that holds and compresses the midgut for *ex vivo* mechanical trigger experiments. **e**, Representative example of three cycles of consecutive mechanical activation. Number of Ca^{2+} cells is plotted over time. Green, compression period; yellow, relaxation period. **f**, Average GCaMP activity during compression from control, $Piezo^{KO}$, *Piezo-i*, *SERCA-i* and *Stim-i* + *InsP3R-i* flies. **g**, Model for mechanical regulation of enteroendocrine precursor differentiation in the fly midgut. Ca^{2+} has different roles in ISCs (proliferation) and enteroendocrine precursors (differentiation). dpErk, extracellular signal-regulated kinase (also known as Rl). Data are mean and s.e.m. *P* values are from a two-tailed Student's *t*-test. Scale bars, 10 mm (**a**) and 50 μm (**b**).

tract by feeding flies with food containing the indigestible fibre methylcellulose, which is a widely used food thickener and ingredient for cell culture. This methylcellulose food induces an 'over-full' phenotype, as fly midguts from approximately 10–15% of flies after 4–5 days of methylcellulose feeding showed a significant increase in diameter (Fig. 4a, Extended Data Fig. 8). Midguts with increased diameter showed a significant increase in the number of Esg^+ cells and EEs (Fig. 4b, c), as well as $Piezo^+$ enteroendocrine precursor cells (Extended Data Fig. 8g–j). This effect is blocked by either *Piezo* knockdown or the null mutant (*Piezo* RNAi or $Piezo^{KO}$, respectively) (Fig. 3b, c, Extended Data Fig. 8k, l). Live-cell imaging of Ca^{2+} activities shows an increase of average Ca^{2+} levels in methylcellulose-fed flies, suggesting that the phenotype is related to increased Ca^{2+} levels (Extended Data Fig. 8n–q, Supplementary Video 4). Indeed, this over-full phenotype is blocked by reducing cytosolic Ca^{2+} (Fig. 4b, c, Extended Data Fig. 8n–q, Supplementary Video 4), suggesting that the mechanical stress generated by the indigestible food promotes EE generation through Piezo activation and subsequent increases in cytosolic Ca^{2+}. As Piezo is mainly enriched in enteroendocrine precursor cells, the increase of stem-cell proliferation may be caused by either a feedback signal from the increased EE generation[25] or low levels of Piezo present in the ISCs.

To test directly whether mechanical forces can activate enteroendocrine precursor cells, we engineered a microfluidic chip that can hold a dissected fly midgut and generate a mechanical compression through controlled air pressure (Fig. 4d, Extended Data Fig. 9a–d). Using this device, we recorded the calcium signal in Dl^+ stem cells of the fly midguts (*Piezo-GAL4* was tested initially but was not used owing to the low GCAMP6s expression). Significantly more stem cells showed high cytosolic Ca^{2+} upon mechanical compression, and this activation was triggered transiently by the change in tissue shape, as Ca^{2+} activity returned to normal within approximately 20 s, even in the presence of constant compression (Fig. 4e, Supplementary Video 6). This mechanically triggered Ca^{2+} activity is significantly reduced in either $Piezo^{KO}$ or *Piezo* RNAi midguts (Fig. 4e, Extended Data Fig. 9e–g, Supplementary Videos 7, 8). Finally, either increases of cytosolic Ca^{2+} through *SERCA* knockdown or decreases of cytosolic Ca^{2+} through *Stim* and *InsP3R* knockdown render the cells irresponsive to the mechanical stimulus (Fig. 4f, Extended Data Fig. 9h–l, Supplementary Videos 9, 10). These data suggest that Ca^{2+} levels in $Piezo^+$ cells can be regulated by a transient mechanical stimulus, which may be generated by repeated vascular muscle contractions during digestion.

In conclusion, we have demonstrated that a new population of unipotent stem cells (enteroendocrine precursors) can directly sense mechanical signals *in vivo* to adjust their differentiation accordingly, and that this mechanosensing is mediated through Piezo activation and cytosolic Ca^{2+} increase. Our findings suggest a potential direct linkage between food digestion with generation of EEs, which regulate various physiological functions, including stem-cell proliferation, intestinal motility, digestion and appetite[25,26]. Such a mechanism may enable the midgut to respond to particular mechanical challenges and maintain tissue homeostasis.

Online Content Methods, along with any additional Extended Data display items and Source Data, are available in the online version of the paper; references unique to these sections appear only in the online paper.

Received 20 September 2016; accepted 12 January 2018.
Published online 7 February 2018.

1. Vining, K. H. & Mooney, D. J. Mechanical forces direct stem cell behaviour in development and regeneration. *Nat. Rev. Mol. Cell Biol.* **18,** 728–742 (2017).
2. Micchelli, C. A. & Perrimon, N. Evidence that stem cells reside in the adult *Drosophila* midgut epithelium. *Nature* **439,** 475–479 (2006).
3. Ohlstein, B. & Spradling, A. The adult *Drosophila* posterior midgut is maintained by pluripotent stem cells. *Nature* **439,** 470–474 (2006).
4. Li, H. & Jasper, H. Gastrointestinal stem cells in health and disease: from flies to humans. *Dis. Model. Mech.* **9,** 487–499 (2016).
5. Lemaitre, B. & Miguel-Aliaga, I. The digestive tract of *Drosophila melanogaster*. *Annu. Rev. Genet.* **47,** 377–404 (2013).
6. Kim, S. E., Coste, B., Chadha, A., Cook, B. & Patapoutian, A. The role of *Drosophila* Piezo in mechanical nociception. *Nature* **483,** 209–212 (2012).
7. Coste, B. *et al.* Piezo proteins are pore-forming subunits of mechanically activated channels. *Nature* **483,** 176–181 (2012).
8. Coste, B. *et al.* Piezo1 and Piezo2 are essential components of distinct mechanically activated cation channels. *Science* **330,** 55–60 (2010).
9. Volkers, L., Mechioukhi, Y. & Coste, B. Piezo channels: from structure to function. *Pflugers Arch.* **467,** 95–99 (2015).
10. Suslak, T. J. *et al.* Piezo is essential for amiloride-sensitive stretch-activated mechanotransduction in larval *Drosophila* dorsal bipolar dendritic sensory neurons. *PLoS ONE* **10,** e0130969 (2015).
11. Buchon, N. *et al.* Morphological and molecular characterization of adult midgut compartmentalization in *Drosophila*. *Cell Reports* **3,** 1725–1738 (2013).
12. Evans, C. J. *et al.* G-TRACE: rapid GAL4-based cell lineage analysis in *Drosophila*. *Nat. Methods* **6,** 603–605 (2009).
13. Amcheslavsky, A., Jiang, J. & Ip, Y. T. Tissue damage-induced intestinal stem cell division in *Drosophila*. *Cell Stem Cell* **4,** 49–61 (2009).
14. Ohlstein, B. & Spradling, A. Multipotent *Drosophila* intestinal stem cells specify daughter cell fates by differential notch signaling. *Science* **315,** 988–992 (2007).
15. Choi, N. H., Kim, J. G., Yang, D. J., Kim, Y. S. & Yoo, M. A. Age-related changes in *Drosophila* midgut are associated with PVF2, a PDGF/VEGF-like growth factor. *Aging Cell* **7,** 318–334 (2008).
16. Cinar, E. *et al.* Piezo1 regulates mechanotransductive release of ATP from human RBCs. *Proc. Natl Acad. Sci. USA* **112,** 11783–11788 (2015).
17. Pathak, M. M. *et al.* Stretch-activated ion channel Piezo1 directs lineage choice in human neural stem cells. *Proc. Natl Acad. Sci. USA* **111,** 16148–16153 (2014).
18. Li, J. *et al.* Piezo1 integration of vascular architecture with physiological force. *Nature* **515,** 279–282 (2014).
19. Gudipaty, S. A. *et al.* Mechanical stretch triggers rapid epithelial cell division through Piezo1. *Nature* **543,** 118–121 (2017).
20. Deng, H., Gerencser, A. A. & Jasper, H. Signal integration by Ca^{2+} regulates intestinal stem-cell activity. *Nature* **528,** 212–217 (2015).
21. Guo, Z. & Ohlstein, B. Stem cell regulation. Bidirectional Notch signaling regulates *Drosophila* intestinal stem cell multipotency. *Science* **350,** aab0988 (2015).
22. Sallé, J. *et al.* Intrinsic regulation of enteroendocrine fate by Numb. *EMBO J.* **36,** 1928–1945 (2017).
23. De Ford, C. *et al.* The clerodane diterpene casearin J induces apoptosis of T-ALL cells through SERCA inhibition, oxidative stress, and interference with Notch1 signaling. *Cell Death Dis.* **7,** e2070 (2016).
24. Roti, G. *et al.* Complementary genomic screens identify SERCA as a therapeutic target in NOTCH1 mutated cancer. *Cancer Cell* **23,** 390–405 (2013).
25. Amcheslavsky, A. *et al.* Enteroendocrine cells support intestinal stem-cell-mediated homeostasis in *Drosophila*. *Cell Reports* **9,** 32–39 (2014).
26. Harrison, E., Lal, S. & McLaughlin, J. T. Enteroendocrine cells in gastrointestinal pathophysiology. *Curr. Opin. Pharmacol.* **13,** 941–945 (2013).

Supplementary Information is available in the online version of the paper.

Acknowledgements We thank R. Binari, W. Song and C. Villalta for technical support; C. Xu, S. Mohr and D. Doupe for comments on the manuscript; and G. Hasan for sharing reagents. This work was supported by the Damon Runyon Cancer Research Foundation (L.H.) and a grant from the National Institutes of Health (R21DA039582). N.P. is an investigator of the Howard Hughes Medical Institute. G.S. and A.D.T.S. are supported by the National Institutes of Health (P01GM103770).

Author Contributions J.H. and L.H. performed the initial GAL4 expression screen in fly gut. L.H. and N.P. designed the experiments. L.H. performed the Piezo-related experiments and analysed the data. G.S. and A.D.T.S. designed and fabricated the microfluidic chip and together with L.H. optimized the experimental conditions. L.H. and N.P. wrote the manuscript with input from all of the authors.

Author Information Reprints and permissions information is available at www.nature.com/reprints. The authors declare no competing financial interests. Readers are welcome to comment on the online version of the paper. Publisher's note: Springer Nature remains neutral with regard to jurisdictional claims in published maps and institutional affiliations. Correspondence and requests for materials should be addressed to L.H. (lihe@genetics.med.harvard.edu) or N.P. (perrimon@rascal.med.harvard.edu).

Reviewer Information *Nature* thanks L. O'Brien, K. Venkatachalam and the other anonymous reviewer(s) for their contribution to the peer review of this work.

METHODS

***Drosophila* stocks and culture.** The following strains were obtained from the Bloomington *Drosophila* Stock Center: *UAS-mtdTomato3XHA* (BL30124), *UAS-tdTomato* (BL3321, BL3322), *UAS-IVS-NES-jRGECO* (BL63795), *UAS-IVS-GCaMP6s* (BL42746), *UAS-mCherry.CAAX* (BL59021), *UAS-mCherry.nls* (BL38424), *UAS-CsChrimson* (BL55134), *tub-GAL80^{TS}* (BL7016), *UASp-Act5C-mRFP* (BL24778), *UAS-mCD8-GFP* (BL32185), *hsFLP*; *Sco/CyO* (BL1929), *UAS-Stim* (BL41757), *UAS-InsP3R* (BL30742), *PiezoP-GAL4* (with cloned promoter, BL59266), *UAS-O-fut1-i* (BL9377), *UAS-Notch^{ICD}* (BL52008), *UAS-Rpr* (BL5823), *Piezo^{KO}* (BL58770), *UAS-Piezo-GFP/CyO* (BL58772), *UAS-Piezo-GFP/TM6B* (BL58773)[6], *UAS-ttk69-i* (BL26315, BL36748), *Act-*(*FRT.Stop*)*lacZ*, *Ubi-*(*FRT.Stop*)*Stinger/CyO* (isolated from BL51308), and G-Trace fly: *UAS-RedStinger*, *UAS-Flp1.D*; *Ubi-*(*FRT.Stop*)*Stinger/CyO* (BL28280). RNAi lines were as previously reported[20]: *UAS-SERCA-i* (BL25928), *UAS-Stim-i* (BL27263, BL52911), *UAS-InsP3R-i* (BL25937, BL51686), and *UAS-PMCA-i* (BL31572). *UAS-Ras1-i* (106642), *UAS-Yki-i* (104523), *UAS-Piezo-i* (2796), *UAS-ase-i* (108511) and *UAS-ttk69-i* (101980) as previously reported[10,27] were from the Vienna *Drosophila* RNAi Center. *esg-GFP* was from D. Doupe. *Su*(*H*)*Gbe-lacZ* was from P. Saavedra. The fly stock for mosaic analysis, *hsFLP*, *tub-GAL4*, *UAS-nlsGFP*; *FRT40*, *tub-GAL80*, was from K. Kim; *Su*(*H*)*Gbe-GAL4* and *Dl-GAL4* were from S. X. Hou[28], *UAS-Orai* was from G. Hasan, *esg-GAL4*, *UAS-nlsGFP* and *Dl-lacZ* were from laboratory stocks. Flies were reared on standard cornmeal/agar medium supplemented with yeast. Adult flies were entrained in 12 h:12 h light–dark cycles at 25 °C unless specifically stated otherwise.

To prepare methylcellulose food, 10% (w/w) methylcellulose (Sigma-Aldrich, 274429) was added to 5% sucrose solution and stirred until fully dissolved. Adult flies 5–7 days after hatching were water-starved (soaked filter paper) for 1 day at 29 °C, and transferred to vials with methylcellulose or control food (5% sucrose-soaked filter paper). Food was changed every other day. Fly midguts with a considerably enlarged diameter (>50% increase compared with the normal section of the same midgut) were counted as enlarged methylcellulose-fed gut (~10–15% of total dissected midguts).

DAPT (4 μM; Sigma-Aldrich, D5942), bleomycin (10 μg ml^{-1}; Calbiochem, 203408), thapsigargin (0.5 μM; Tocris, 1138) and trametinib (10 μM; Selleckchem, S2673) were used for chemical treatment. All feeding experiments were performed using 5% sucrose-saturated filter paper unless stated otherwise.

For the lineage-tracing experiments[12], the temperature-sensitive GAL80^{TS} transgene was used to suppress the early activity of GAL4 before adulthood. Flies (4–5 days old) were incubated at 32 °C for 1 day to activate GAL4 and then maintained at 25 °C for 7 days. For *Piezo-GAL4*, flies were incubated at 32 °C for 4 days and then maintained at 25 °C for 3 days because of its low activity. Lineage tracing of methylcellulose-fed flies was done by induction of flies for 4–5 days at 32 °C and when feeding the flies on 5% sucrose plus 10% methylcellulose for 4 days at 25 °C. To visualize the GAL4-expressing cells, flies were shifted to 32 °C overnight before analysis. To create random clones using *hsFLP*; *Ubi-*(*FRT.Stop*)*Stinger*, we heat-shocked the 3–4-day-old adult flies at 37 °C for 30 min, and then kept them at 25 °C for 2 weeks.

For the mosaic analysis with a repressible cell marker (MARCM) experiments[29], 4–5-day-old flies were heat-shocked three times at 37 °C for 1 h within 1 day. Then flies were maintained at 25 °C, except for the flies containing RNAi, which were maintained at 32 °C to increase the expression of the double-stranded RNAs. Temperature has no significant effect on the ratio of EEs in the progenies (data not shown). Midguts from female flies were analysed after 14 days. (GFP-positive clones were induced by transient incubation at 32 °C, then flies were kept at 25 °C for 10 days and 32 °C overnight before analysis.)

Immunofluorescence imaging. Immunostaining of *Drosophila* midguts was performed as previously described[30]. The following primary antibodies were used: mouse anti-Prospero (1:50; Developmental Studies Hybridoma Bank, MR1A), rabbit anti-phospho-histone H3 (1:1,000; Millipore, 06–570); mouse anti-haemagglutinin (Abcam, ab18181), rabbit anti-dpErk1/2 (1:500; Cell Signaling, 4370), mouse anti-Delta (1:50; Developmental Studies Hybridoma Bank, C594.9B), mouse anti-β-galactosidase (1:400; Promega, Z3781), rabbit anti-tachykinin (1:5,000: ref. 31). Secondary antibodies were goat anti-rabbit and anti-mouse IgGs conjugated to Alexa 555 and Alexa 647 (used at 1:500, Thermo Fisher Scientific, A-21428, A-21244, A-21235, A-21422). Fly guts were mounted in Vectashield with DAPI (Vector Laboratories). In all micrographs, blue staining shows the nuclear marker DAPI. Fluorescence micrographs were acquired with a Zeiss LSM 780 confocal microscope. All images were adjusted and assembled in NIH ImageJ.

CRISPR–Cas9 genome editing. Guide RNAs (gRNAs) targeting the start codon of *Piezo* were designed using the 'find CRISPRs' online tool (http://www.flyrnai.org/crispr2/)[32,33]. The genome-editing efficiency of different candidate gRNAs was tested in tissue culture using T7 endonuclease assay[34], and the following sequence with highest cutting efficiency was used: CTGGAGGAGAACGGCGCCGG.

Genomic fragments approximately 1 kb from the upstream and downstream of the start codon were amplified from fly genome using the following primers: upstream forward: 5′-CTTCGGTACCGGATCACTGTGCATGTGAGGCATTA-3′, upstream reverse: 5′-GCTTCATTTTGGATCACTCAGACTCCGACTCCAAC-3′; downstream forward: 5′-CGGCGGCCGCTCTAGTCAGCTATGCGTGCATGGT-3′, downstream reverse: 5′-AAGCTGGGTGTCTAGGGGAATGTGGTAGGCAAACTA-3′.

Genomic fragments were cloned upstream and downstream of GAL4-SV40 in pENTR vector by In-fusion (Clontech) to make the donor construct.

For CRISPR–Cas9-mediated homologous recombination, gRNA in pCFD3 (0.2 μg μl^{-1}) and donor DNA (0.5 μg μl^{-1}), were co-injected into the embryos of *nos-Cas9/attP2* flies[35]. Knock-in flies were selected by genomic PCR using following primers from insertion and *Piezo* gene: upstream forward: 5′-CCCACAATTTCGCACTCTTT-3′, upstream reverse: 5′-GTCTTCACGGGGAAAAATGA-3′; downstream forward: 5′-GTGGTTTGTCCAAACTCATCAATG-3′, downstream reverse 5′-CGGACAGCAGGAAAATGAGA-3′.

Piezo-GAL4 knock-in homozygous flies are viable and fertile. Quantitative PCR (qPCR) of whole adult flies showed that *Piezo* mRNA from homozygous *Piezo-GAL4* knock-in flies was reduced by ~50% compared to *Piezo-GAL4/CyO*. The mRNA of *Piezo* from *Piezo-GAL4/CyO* was not significantly different from wild-type flies. Also, qPCR of *Piezo^{KO}* (BL58770) is consistent with this allele being a complete null[6] as it showed a more than 95% reduction of *Piezo* mRNA.

Optogenetic activation of CsChrimson in fly midgut. Red-shifted channelrhodopsin CsChrimson[36] was used to increase cytosolic Ca^{2+} in stem cells by light. *UAS-CsChrimson* was expressed using either *Dl-GAL4* or *Piezo-GAL4*. All crosses and the early development of flies were performed under dark conditions at 18 °C. The experiment was done at 25 °C. Adult flies were kept either on 2% agarose containing 5% sucrose and 1% yeast extract in the dark, or on 2% agarose containing 5% sucrose, 1% yeast extract and 50 mM all-trans-retinal (ATR) in the presence of orange–red light from LED. Two 1-metre SMD5050 RGB LED strips (total power ~2 × 4 W, eTopxizu) was attached to the inner wall of a cylinder chamber (~10 cm in diameter and 15 cm in height) covered by aluminium foil to enhance the light intensity (Extended Data Fig. 7a). The RGB LED strip was set at constant maximal brightness with green (500–560 nm) and red (600–650 nm) LED units on (estimated light intensity ~ 2.5 mW cm^{-2}). The power of the LED is controlled manually to maintain 12 h/12 h on/off circadian rhythms. Flies were kept under the indicated condition for 2 weeks before analysis.

Calcium imaging. Cytosolic Ca^{2+} was monitored in ISCs using the red fluorescent indicator RGECO[37]. GFP was used as an internal control and an indicator of stem cells and enteroblasts. Young adult flies (4–5 days after eclosion) were first incubated at 32 °C for 5–7 days before the experiment. For live-cell imaging experiment, dissected intact midgut was cultured in adult-hemolymph-like (AHL) medium plus 2% fetal bovine serum (FBS). The addition of FBS into the AHL moderately increases the average cytosolic Ca^{2+} level and reduced the oscillation frequency, but allows a longer maintenance of dissected midgut under normal condition up to 5–6 h. Air-permeable lummox dish (SARSTEDT, 94.6077.331) was used as the imaging device as previously described[38]. Images of anterior midgut area were captured on Zeiss LSM 780 confocal microscope equipped with definite focus using Plan-Neofluar 25×/oil numerical aperture (NA) 0.8 lens. A *z*-stack of dual-colour images (488 nm excitation/500–550 nm detection for GFP, and 561 nm excitation/580–650 nm detection for RGECO) was recorded every 20 s. Both colour channels were recorded simultaneously with line-based scanning. Images were manually analysed in NIH ImageJ.

Microfluidic chip design and operation. The fly gut was immobilized and force stimuli were applied in a microfluidic chip. The design took advantage of the pressure sensitivity of the poly material (PDMS, the building materials of the microfluidics), and had been applied in previous studies of *Caenorhabditis elegans*[39]. The chip was designed using the software of Tanner L-Edit and fabricated following standard microfluidics fabrication procedures[40]. The layout of the design is shown in Extended Data Fig. 9. The middle channel was designed for loading and holding the gut, with a size of 6 mm long and 200 μm wide. The two side channels delivered the pressure, with a size of 1 mm long and 450 μm width. The membrane in between is 70 μm wide, and was used for squeezing the guts when pressures were applied. The pattern was transferred onto a silicon wafer via photoresist with the height of 200 μm, which was then transferred to PDMS and bonded with glass. To achieve the desired softness, the PDMS was mixed 20:1 with the cross-linker.

Freshly dissected fly midguts were loaded in the channel inlet with the anterior part of the gut located in the middle between the two membranes. In the device, compressed air is connected to the side channels via a bidirectional switch. In the off state, the side channels are at the atmospheric pressure, and no pressure is applied to the gut. When switched to the on state, compressed air presses the PDMS membrane and squeezes the gut. The ratio of the channel width reduction was ~30% during the compression and the relaxation time of the PDMS membrane

was ~1 s. Ca^{2+} signals were indicated by GCAMP6s[41] and captured using a Zeiss LSM 780 confocal microscope equipped with a definite focus using Plan-Neofluar 10×/0.30 lens. The anterior midgut area was recorded as time-lapse of *z*-stacks capturing the whole depth of the midgut every 2 s. GCAMP6s emission was excited at 448 nm and recorded at 500–550 nm and tdTomato was excited at 561 nm and recorded at 580–610 nm. Ca^{2+} imaging experiments were done with identical acquisition parameters for consistency. Images from the experiment were projected using maximum intensity projection and analysed using a macro in ImageJ to automatically detect the number of GFP-positive cells in each frame. Tracing of Ca^{2+} signals in individual stem cells was done using the *Z*-axis profiling function of NIH ImageJ. The Ca^{2+} signal in individual stem cells during mechanical compression was tacked manually.

qPCR. Total RNA was extracted from 5–7-day-old female by TRIZOL reagent (Thermo Fisher Scientific), converted to cDNA template after DNase I treatment and purification using QIAGEN RNeasy kit. qPCR was performed using SYBR Green with *Gapdh1* and *αTub84B* as internal controls. *Piezo* mRNA was detected by two pairs of independent primers (Supplementary Table 2).

Statistics and reproducibility. All the images presented and used for quantification are from the anterior region of adult female fly midgut for consistency. Two or three square areas (10,000 μm^2 unless specified otherwise) were randomly selected from each midgut and quantified automatically using the cell counting function of NIH ImageJ. All experiments were independently biologically repeated twice (unless specified otherwise) with similar results presented in the figures. No randomization or blinding was used. Statistical analysis was performed using Microsoft Excel. All *P* values were determined by two-tailed Student's *t*-test with unequal variances. Sample sizes were chosen empirically based on the observed effects and listed in the figure legends.

Data availability. All relevant data have been included in the paper and its Supplementary Information. Original quantifications of different cell numbers are listed in the Supplementary Data. Complete genotypes information is provided in Supplementary Table 1. Original data that support the findings of this study are available from the corresponding author upon request.

27. Xu, C., Luo, J., He, L., Montell, C. & Perrimon, N. Oxidative stress induces stem cell proliferation via TRPA1/RyR-mediated Ca^{2+} signaling in the *Drosophila* midgut. *eLife* **6,** e22441 (2017).
28. Zeng, X., Chauhan, C. & Hou, S. X. Characterization of midgut stem cell- and enteroblast-specific GAL4 lines in *Drosophila*. *Genesis* **48,** 607–611 (2010).
29. Lee, T. & Luo, L. Mosaic analysis with a repressible cell marker (MARCM) for *Drosophila* neural development. *Trends Neurosci.* **24,** 251–254 (2001).
30. Karpowicz, P., Perez, J. & Perrimon, N. The Hippo tumor suppressor pathway regulates intestinal stem cell regeneration. *Development* **137,** 4135–4145 (2010).
31. Veenstra, J. A., Agricola, H. J. & Sellami, A. Regulatory peptides in fruit fly midgut. *Cell Tissue Res.* **334,** 499–516 (2008).
32. Housden, B. E. *et al.* Identification of potential drug targets for tuberous sclerosis complex by synthetic screens combining CRISPR-based knockouts with RNAi. *Sci. Signal.* **8,** rs9 (2015).
33. Housden, B. E., Hu, Y. & Perrimon, N. Design and generation of *Drosophila* single guide RNA expression constructs. *Cold Spring Harb. Protoc.* http://doi.org/10.1101/pdb.prot090779 (2016).
34. Housden, B. E., Lin, S. & Perrimon, N. Cas9-based genome editing in *Drosophila*. *Methods Enzymol.* **546,** 415–439 (2014).
35. Ren, X. *et al.* Optimized gene editing technology for *Drosophila melanogaster* using germ line-specific Cas9. *Proc. Natl Acad. Sci. USA* **110,** 19012–19017 (2013).
36. Klapoetke, N. C. *et al.* Independent optical excitation of distinct neural populations. *Nat. Methods* **11,** 338–346 (2014).
37. Zhao, Y. *et al.* An expanded palette of genetically encoded Ca^{2+} indicators. *Science* **333,** 1888–1891 (2011).
38. Dai, W. & Montell, D. J. Live imaging of border cell migration in *Drosophila*. *Methods Mol. Biol.* **1407,** 153–168 (2016).
39. Wen, Q. *et al.* Proprioceptive coupling within motor neurons drives *C. elegans* forward locomotion. *Neuron* **76,** 750–761 (2012).
40. McDonald, J. C. *et al.* Fabrication of microfluidic systems in poly(dimethylsiloxane). *Electrophoresis* **21,** 27–40 (2000).
41. Chen, T. W. *et al.* Ultrasensitive fluorescent proteins for imaging neuronal activity. *Nature* **499,** 295–300 (2013).
42. Micchelli, C. A., Sudmeier, L., Perrimon, N., Tang, S. & Beehler-Evans, R. Identification of adult midgut precursors in *Drosophila*. *GEP* **11,** 12–21 (2011).
43. Wang, C., Guo, X., Dou, K., Chen, H. & Xi, R. Ttk69 acts as a master repressor of enteroendocrine cell specification in *Drosophila* intestinal stem cell lineages. *Development* **142,** 3321–3331 (2015).

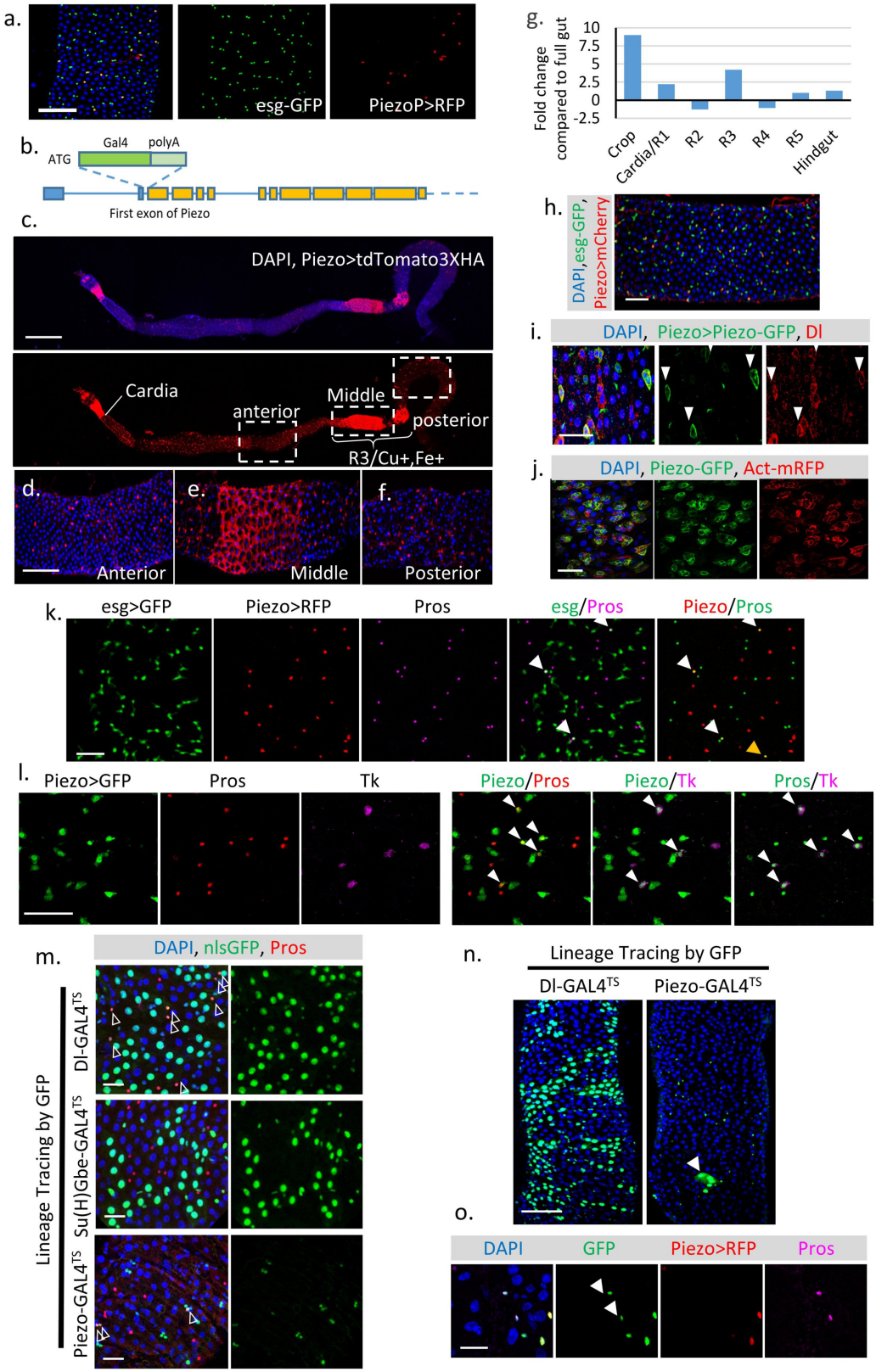

Extended Data Figure 1 | See next page for caption.

Extended Data Figure 1 | Piezo expression pattern and Piezo$^+$ cell lineage in the fly midgut. a, Expression pattern of GAL4 (BL59266) driven by the *Piezo* promoter[6]. **b**, Schematic of *Drosophila Piezo* gene structure. *GAL4* and the polyA tail were knocked in after the first start codon of *Piezo*; we refer to this knock-in GAL4 line as *Piezo-GAL4*. The ten predicted *Piezo* isoforms share the same N terminus. **c**–**f**, *Piezo* expression pattern in the midgut (*Piezo-GAL4*, *UAS-tdTomato3XHA*). Tissue was stained with an anti-haemagglutinin (HA) antibody to enhance the original signal. In addition to the small diploid stem cells, *Piezo* is also expressed in enterocytes after the cardia and around the copper and iron regions of the midgut. GAL4 activity outside the intestinal epithelium from tracheal cells can also be detected. **g**, Expression pattern of *Piezo* mRNA along different sections of the midgut. **h**, *Drosophila* midgut with Piezo$^+$ cells labelled by mCherry (*Piezo-GAL4*, *UAS-mCherry*; red) and Esg$^+$ cells labelled by *esg-GFP* (green). **i**, Midgut with Piezo$^+$ cells labelled by GFP (*Piezo-GAL4*, *UAS-Piezo-GFP*; green). Dl$^+$ stem cells were stained with an anti-Dl antibody (red). Arrowheads denote Piezo cells. **j**, Midgut expressing Piezo (GFP$^+$, green) in Esg$^+$ cells, with F-actin labelled by *UASp-Act5C-mRFP* (red). Piezo may form large cytoplasmic aggregates under stressed conditions[19], however, in the fly midgut, the GFP-tagged Piezo protein is localized primarily on the plasma membrane under both quiescent and over-proliferation conditions (**i**, **j**). **k**, *esg-GFP* is used as an indicator of newborn EEs. Under normal physiological conditions, around 2–3% of Esg$^+$ cells are also positive for Pros, suggesting that they are either differentiating or have just differentiated into EEs (denoted by arrowheads). All the newborn EEs are also positive for Piezo. Piezo and Pros double-positive but Esg-negative cells can be found occasionally (yellow arrowhead), most probably reflecting their late stage of differentiation. **l**, Piezo$^+$ newborn EEs are composed of both tachykinin-positive (Tk$^+$) and Tk$^-$ cells, suggesting that Piezo$^+$ cells are precursors for different types of EE. Arrowheads denote cells positive for both Piezo and Pros (left), Piezo and Tk (middle) or Pros and Tk (right). **m**, Dl$^+$, Su(H) Gbe$^+$ and Piezo$^+$ cells were traced using *Dl-GAL4*, *Su(H)Gbe-GAL4* and *Piezo-GAL4*. Arrowheads denote Pros (red) and GFP double-positive cells. **n**, Compared with *Dl-GAL4^{TS}*, which generates large GFP$^+$ enterocyte clones, *Piezo-GAL4^{TS}* primarily generates individual GFP$^+$ cells, with the occasional GFP$^+$ enterocyte cell clone (arrowhead). **o**, To visualize cells with GAL4 activity, which is repressed by the presence of *tub-GAL80^{TS}*, we incubated flies at 32 °C overnight before analysis. In this panel, two Pros$^+$ cells are GFP-positive but RFP-negative (indicated by arrowheads), suggesting that they are derived from Piezo$^+$ cells and then stop expressing Piezo. All experiments were independently repeated at least twice with similar results. Scale bars, 50 μm (**a**, **h**, **n**); 500 μm (**c**), 100 μm (**d**–**f**), 25 μm (**i**, **j**), 20 μm (**k**–**m**), 10 μm (**o**).

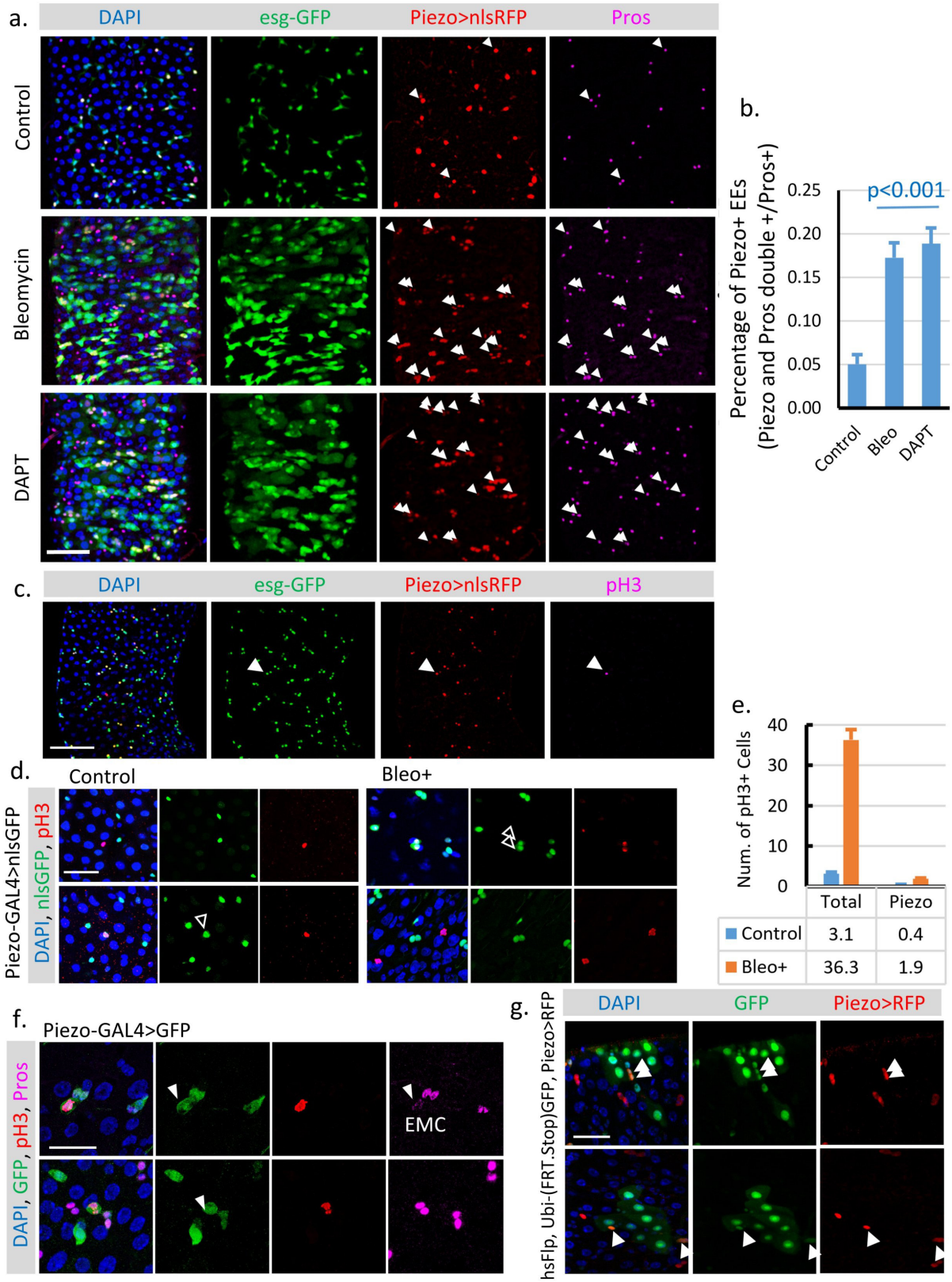

Extended Data Figure 2 | See next page for caption.

Extended Data Figure 2 | Piezo$^+$ enteroendocrine precursors are ISC-derived EE precursors with reduced mitotic ability. a, Midguts from flies treated with bleomycin (10 μg ml^{-1} in 5% sucrose) or the γ-secretase inhibitor DAPT (4 mM in 5% sucrose). Arrowheads denote cells positive for both Piezo and Pros. Most (>95%) Piezo and Pros double-positive cells are also positive for Esg, suggesting that these cells are newborn EEs that still retain the *esg-GFP* signal. **b**, Percentage of newborn EEs (Piezo and Pros double-positive cells versus total Pros$^+$ EEs) in fly midguts under control, bleomycin and DAPT treatments. Cells within 200 μm × 200 μm areas, $n = 27$ (control), $n = 25$ (bleo), and $n = 22$ (DAPT), were analysed. **c**, Midgut with stem cells labelled by *esg-GFP* (green), Piezo$^+$ cells labelled by RFP (red), and mitotic cells labelled by anti-pH3 (magenta; arrowhead). **d**, **e**, Representative images of midguts from flies fed on either control (5% sucrose) or bleomycin (5% sucrose plus 10 μg ml^{-1} bleomycin) food. Piezo$^+$ enteroendocrine precursor cells are labelled by GFP (green), mitotic cells are labelled by pH3 staining (red). Arrowheads denote mitotic Piezo$^+$ cells. Because all pH3$^+$ cells are Dl$^+$ cells (according to the *Dl-lacZ*-labelled midgut), we counted all Piezo$^-$ pH3$^+$ cells as pH3$^+$ ISCs. Under both control (5% sucrose) and damage (5% sucrose + 10 μg ml^{-1} bleomycin) conditions, only around 8–10% of the pH3$^+$ cells are Piezo$^+$ (~40% of total Dl$^+$ cells), suggesting that Piezo$^+$ cells are significantly less mitotically active than Piezo$^-$ Dl$^+$ cells. **f**, Around 50% of pH3$^+$ Piezo$^+$ cells show low levels of Pros staining. In addition, all pH3$^+$ Pros$^+$ cells are positive for Piezo, suggesting that Piezo$^+$ enteroendocrine precursor cells represent more general EE precursor cells than 'enteroendocrine mother cells' (EMCs)[21]. Arrowheads denote mitotic Piezo$^+$ cells. All experiments were independently repeated at least twice with similar results. **g**, Random GFP$^+$ clones were generated using *hsFLP*; *Ubi-*(*FRT.Stop*)*GFP/Piezo-GAL4*; *UAS-nlsRFP*. Flies (3–4 days old) were heat-shocked at 37 °C for 30 min once to induce clones in ISCs. The flies were then kept at 25 °C for 2 weeks before analysis. Within each GFP$^+$ clone, which is derived from ISCs, there are typically 1–2 Piezo$^+$ cells in the cluster (arrowheads), suggesting that Piezo$^+$ cells are generated from ISCs after adulthood. All experiments were independently repeated at least twice with similar results. Data are mean + s.e.m. *P* values are from a two-tailed Student's *t*-test with unequal variance. Scale bars, 50 μm (**a**, **c**), 20 μm (**d**, **f**) and 25 μm (**g**).

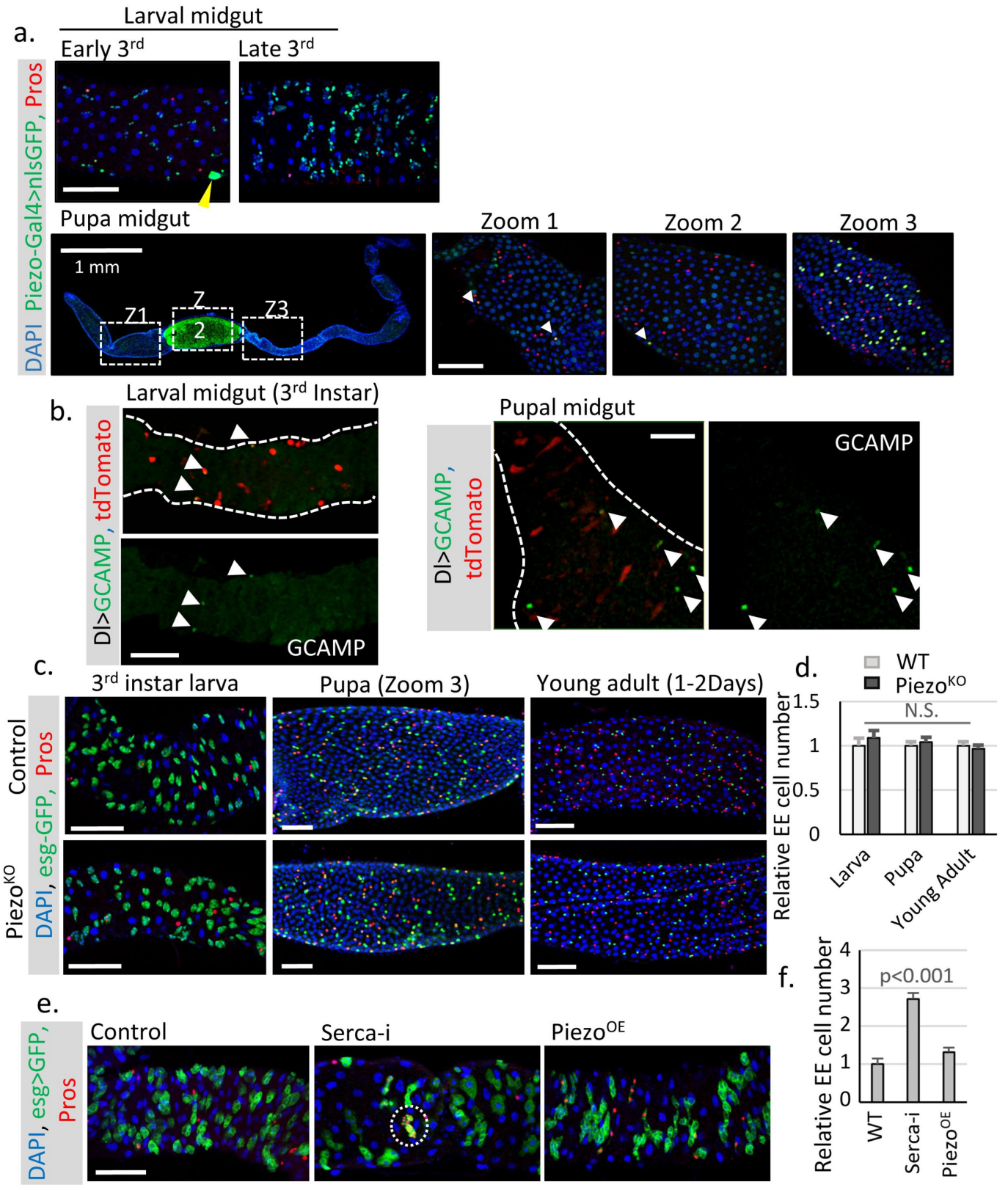

Extended Data Figure 3 | See next page for caption.

Extended Data Figure 3 | Expression and function of Piezo in larval and pupal midguts. a, Piezo^{+} cells are labelled by GFP. Piezo is enriched in adult midgut precursor cells during larval stages. Strong expression of Piezo is also detected in tracheal cells associated with the midgut (yellow arrowhead denotes tracheal cell nucleus). After pupariation, the GFP signal can be detected at low levels in most midgut cells (including enterocytes), but is enriched in a few stem cells and EEs, which presumably are newborn EEs. Pupal gut 72 h after pupa formation is shown, with arrowheads denoting cells positive for both Piezo and Pros. High levels of Piezo are detected in a large number of EEs present in the pupal midgut, suggesting that the association of Piezo expression and EE differentiation is conserved during the pupal stage. **b**, Live imaging of larval and pupal midguts expressing GCAMP and tdTomato by *Dl-GAL4*. Arrowheads denote cells with high GCAMP activity. **c**, **d**, Midguts from *Piezo*-null (*Piezo*^{KO}) flies show no significant defects in EE generation during larval, pupal or early adult stages (1–2 days after eclosion). Number of midgut areas quantified: $n = 24$ (WT, larva), $n = 23$ (WT, pupa), $n = 28$ (WT, young adult), $n = 23$ (*Piezo*^{KO}, larva), $n = 23$ (*Piezo*^{KO}, pupa), $n = 28$ (*Piezo*^{KO}, young adult). These results indicate that mechanically controlled Piezo activation is not the major mechanism for EE production during early development. Unlike the adult midgut, the larval midgut does not regenerate through mitosis and only grows through increases in cell size. It is only during late stages of third instar larval development that the quiescent adult midgut precursor cells start to proliferate and generate both new enterocytes and EEs for pupal gut formation, and most new EEs (~several hundred) are created within a very narrow time window approximately 72–96 h after pupa formation[42]. Therefore, the generation of EEs is 15–30 times faster at that stage than during the adult stage under physiological condition, suggesting that a different mechanism that stimulates strong acute EE differentiation is involved during developmental stages. **e**, **f**, Knockdown of SERCA using *esg-GAL4* during larval stages significantly increases EE cell number. Conversely, overexpression of *Piezo* (*Piezo*^{OE}) has no significant phenotype. White circle denotes a cluster of extra EE cells. Number of midgut areas quantified: $n = 26$ (WT), $n = 28$ (*SERCA-i*), $n = 26$ (*Piezo*^{OE}). All experiments were independently repeated at least twice with similar results. Data are mean + s.e.m. *P* values are from a two-tailed Student's *t*-test with unequal variance. Scale bars, 50 μm.

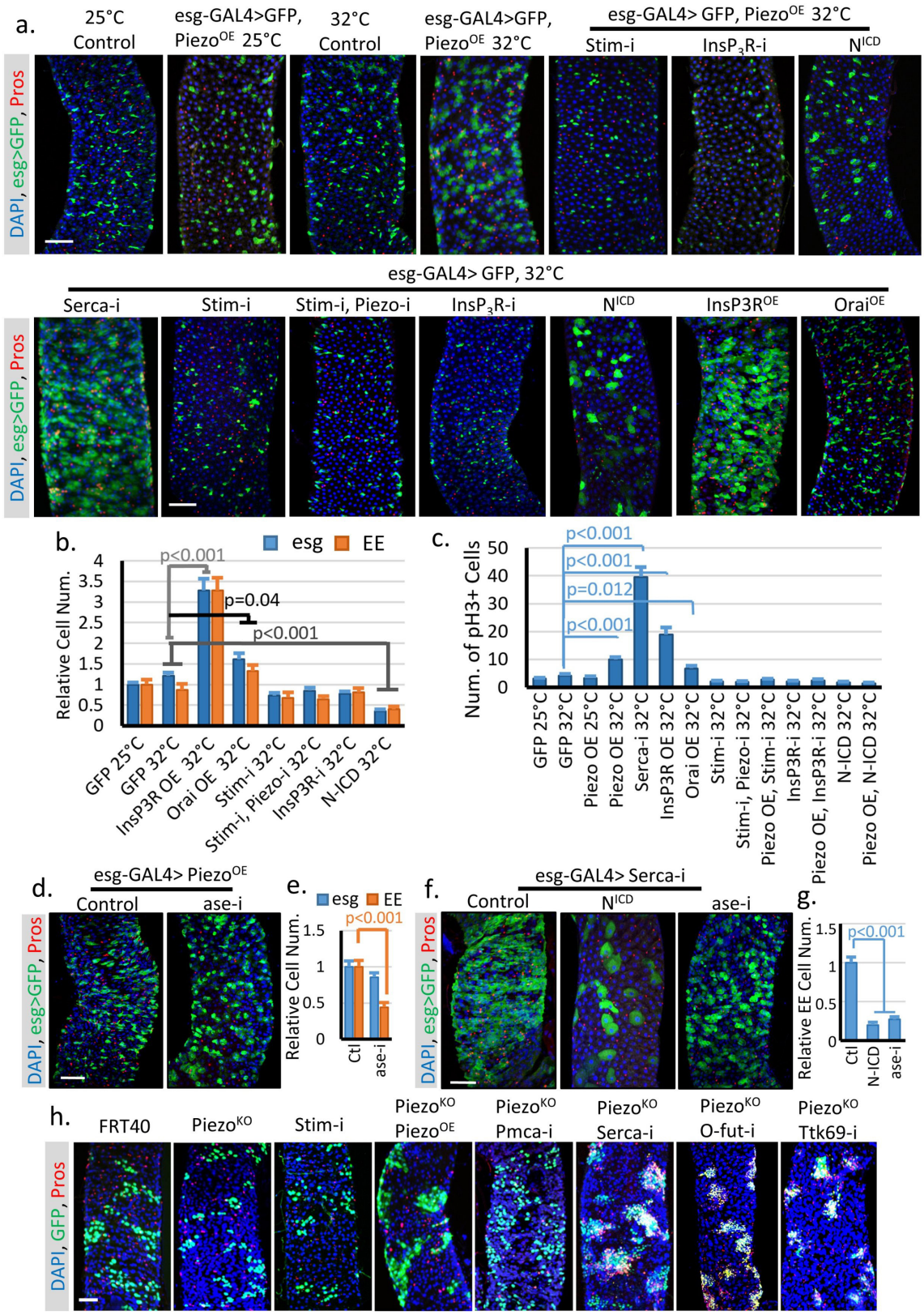

Extended Data Figure 4 | See next page for caption.

Extended Data Figure 4 | Piezo regulates stem-cell differentiation primarily through Ca^{2+} signalling, which is upstream of Notch, Ttk69 and the *achaete-scute* gene complex (AS-C). a, Phenotypes associated with *UAS-GFP* (at 25 °C or 32 °C), *UAS-Piezo*^{OE} together with *Stim-i*, *InsP3R-i* and N^{ICD}, and *UAS-GFP* together with *Stim-i*, *Stim-i* + *Piezo-i*, *InsP3R-i*, N^{ICD}, *InsP3R* overexpression (*InsP3R*^{OE}), and *Orai*^{OE} (at 32 °C). Overexpression of *Piezo* using *esg-GAL4* did not show a significant phenotype at 25 °C. By contrast, incubation at 32 °C for 4 days showed an increased in the number of both Esg^+ cells and $Pros^+$ EEs. Moderate overexpression of *Piezo* at 25 °C had no significant effects. However, strong overexpression at 32 °C caused an increase in both Esg^+ cells and EEs, which phenocopied the increase of cytosolic Ca^{2+} through SERCA reduction. All flies were incubated at the indicated temperature for 4–5 days before analysis. **b**, The number of Esg^+ and $Pros^+$ cells within 10,000-μm^2 area. Number of midgut areas quantified: $n = 30$ (GFP 25 °C), $n = 31$ (GFP 32 °C), $n = 25$ (*InsP3R*^{OE} 32 °C), $n = 27$ (*Orai*^{OE} 32 °C), $n = 31$ (*Stim-i* 32 °C), $n = 27$ (*Stim-i*, *Piezo-i* 32 °C), $n = 29$ (*InsP3R-i* 32 °C), $n = 29$ (N^{ICD} 32 °C). **c**, Average number of mitotic cells within the fly midgut from indicated genotypes. Number of midguts analysed: $n = 20$ (GFP 25 °C), $n = 19$ (GFP 32 °C), $n = 20$ (*Piezo*^{OE} 25 °C), $n = 19$ (*Piezo*^{OE} 32 °C), $n = 18$ (*SERCA-i*, 32 °C), $n = 18$ (*InsP3R*^{OE} 32 °C), $n = 24$ (*Orai*^{OE} 32 °C), $n = 19$ (*Stim-i,* 32 °C), $n = 19$ (*Stim-i*, *Piezo-i* 32 °C), $n = 19$ (*Piezo*^{OE}, *Stim-i*, 32 °C), $n = 18$ (*InsP3R-i* 32 °C), $n = 18$ (*Piezo*^{OE}, *InsP3R-i* 32 °C), $n = 17$ (N^{ICD} 32 °C), $n = 17$ (*Piez*^{OE}, N^{ICD} 32 °C). **d**, **e**, EE production induced by overexpression of *Piezo* is blocked by RNAi that targets the *acheate-scute* complex (AS-C) component *asense* (*ase*). Number of midgut areas quantified: $n = 29$ (ctl), $n = 30$ (*ase-i*). **f**, **g**, Expression of N^{ICD} in the presence of *SERCA-i* significantly reduced both stem-cell proliferation and EE production. Knockdown of *ase* specifically blocks EE differentiation but not proliferation. Number of midgut areas quantified: $n = 27$ (ctrl), $n = 24$ (N^{ICD}), $n = 25$ (*ase-i*). Even though *ttk69* (also known as *ttk*) and *AS-C* knockdown affect Piezo- and SERCA-related phenotypes, Ca^{2+} signalling probably does not directly affect Ttk69 or *AS-C*; previous studies have shown that Ttk69 and AS-C reduction can convert Notch-high enteroblasts into EEs[43], but neither *Piezo* overexpression nor *SERCA* knockdown has any effect in enteroblasts. **h**, MARCM clones of cells homozygous for FRT (control), *Piezo*^{KO}, *Stim-i*, *Piezo*^{KO} + *Piezo*^{OE}, *Piezo*^{KO} + *PMCA-i*, *Piezo*^{KO} + *SERCA-i*, *Piezo*^{KO} + *O-fut1-i*, and *Piezo*^{KO} + *ttk69-i*. Rescue/reversion of the reduction of EEs in *Piezo*-null clones by increasing levels of cytosolic Ca^{2+} (by knocking down the Ca^{2+} export pump PMCA or endoplasmic reticulum Ca^{2+} ATPase SERCA) or by reducing Notch activity (by knocking down its key processing enzyme O-fut1, and knocking down EE cell fate repressor Ttk69). All data are from at least two independent replicates and are expressed as mean + s.e.m. *P* values are from a two-tailed Student's *t*-test with unequal variance. Scale bars, 50 μm.

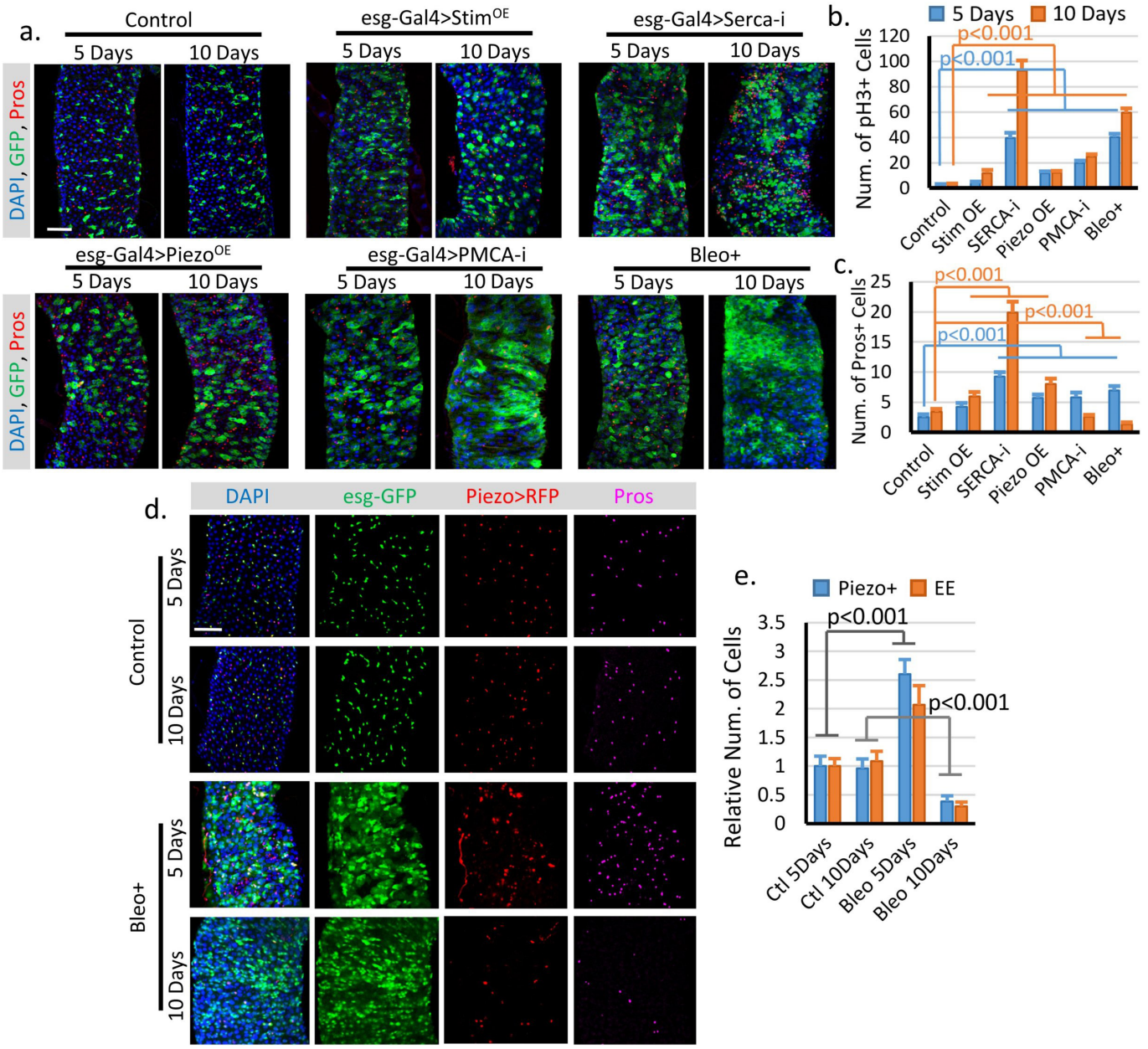

Extended Data Figure 5 | Prolonged increase of stem-cell proliferation may reduce EE cell number. a, Fly midguts of each indicated genotype/condition were analysed after incubation for 5 and 10 days at 32 °C. Esg^+ cells (GFP^+, green) and EE cells ($Pros^+$, red). Representative images from two independent replicates. **b**, Quantification of mitosis ($pH3^+$ cell number) of midguts from flies expressing GFP only (control, $n = 16$ (5 days), $n = 16$ (10 days)), full-length *Stim* ($Stim^{OE}$, $n = 15$ (5 days), $n = 17$ (10 days), *SERCA-i* ($n = 18$ (5 days), $n = 16$ (10 days)), $Piezo^{OE}$ ($n = 17$ (5 days), $n = 18$ (10 days)), *PMCA-i* ($n = 15$ (5 days), $n = 15$ (10 days)), and flies fed bleomycin-containing food (regular food + 10 μg ml^{-1} bleomycin, $n = 15$ (5 days), $n = 13$ (10 days)). **c**, Quantification of $Pros^+$ EE cell number from 10,000-μm^2 regions: $n = 31$ (5 days), $n = 30$ (10 days) (control); $n = 30$ (5 days), $n = 32$ (10 days) ($Stim^{OE}$); $n = 30$ (5 days), $n = 30$ (10 days) (*SERCA-i*); $n = 31$ (5 days), $n = 32$ (10 days) ($Piezo^{OE}$); $n = 32$ (5 days), $n = 31$ (10 days) (*PMCA-i*); $n = 29$ (5 days), $n = 28$ (10 days) (Bleo+). Bleomycin treatment or *PMCA-i* significantly reduced the number of EEs. This reduction is primarily due to increased turnover of EEs, as blocking cell mitosis for 5 days had no significant effect on EE cell number (Extended Data Fig. 7). The differences between stem-cell proliferation and EE differentiation may be due to a different level of cytosolic Ca^{2+} increase and the Ca^{2+} depletion in the ER store. **d**, Change of $Piezo^+$ cells and EEs after 5 and 10 days of control (5% sucrose) or bleomycin (5% sucrose plus 10 μg ml^{-1} bleomycin) treatment. Representative images from two independent replicates. **e**, Quantification of $Piezo^+$ cells and EEs from 10–15 midguts for each condition. Both $Piezo^+$ cells and EEs number increased after 5 days of bleomycin treatment, and significantly decreased after 10 days of treatment. Cell numbers were quantified within a 10,000-μm^2 area, except for pH3, which is quantified from the whole midgut. All data are mean + s.e.m. *P* values are from a two-tailed Student's *t*-test with unequal variance. Scale bars, 50 μm.

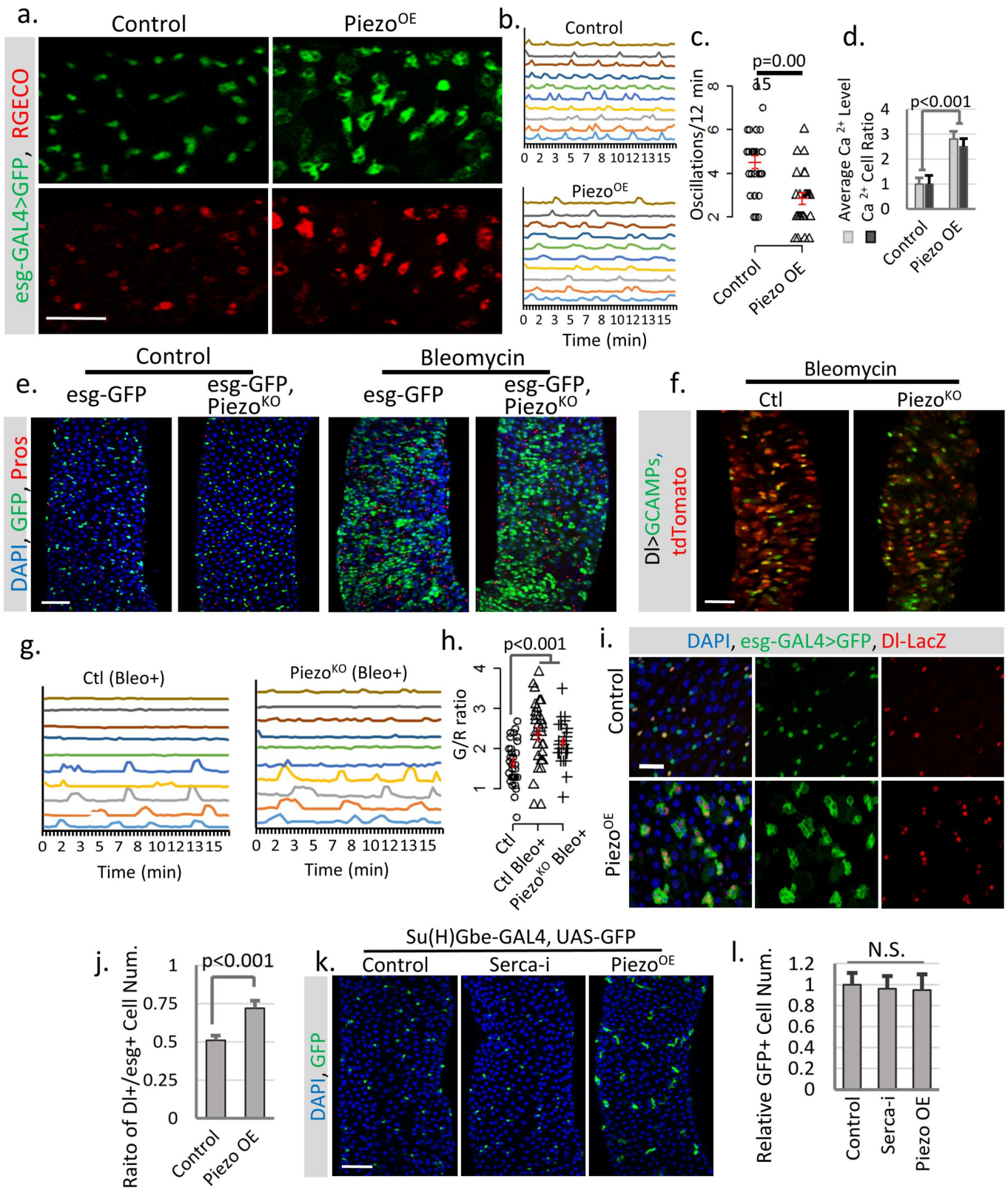

Extended Data Figure 6 | See next page for caption.

Extended Data Figure 6 | *Piezo* overexpression increases cytosolic Ca^{2+} levels, which further triggers proliferation of ISCs but not enteroblasts. **a**, Overexpression of *Piezo* in Esg^+ (GFP^+, green) cells at 32 °C causes an increase in cytosolic Ca^{2+} (indicated by the red fluorescent calcium reporter RGECO) compared to control (*esg-GAL4/UAS-GFP*, *UAS-RGECO*). Representative images from three short time-lapse imagings of cultured fly midguts. Scale bar, 50 μm. **b**, Typical traces of Ca^{2+} oscillations in Esg^+ cells of midgut from either control or $Piezo^{OE}$ flies from three independent replicates. **c**, Ca^{2+} oscillation frequency of Esg^+ cells from either control or *Piezo* overexpression midguts. Data are from 27 cells from three replicates for each condition. **d**, Average RGECO signal intensity in all GFP^+ cells (blue) and percentage of Ca^{2+}-positive cells (signal higher than 3× the s.d. of background) compared to total GFP^+ cells (orange). Signal intensities were calculated from 10,000-μm^2 regions: $n = 17$ (control), $n = 22$ ($Piezo^{OE}$) from three independent experiments. **e**, Bleomycin (10 μg ml^{-1}) (5 days of treatment) triggers a significant increase in Esg^+ cells and EE cells in both wild-type and $Piezo^{KO}$ flies. Representative images from three independent replicates are shown. **f**, Images of live midguts from wild-type and $Piezo^{KO}$ flies. Flies were fed on food containing bleomycin for 3 days before imaging. **g**, **h**, Traces of Ca^{2+} oscillations in Dl^+ stem cells from wild-type and *Piezo* mutant flies fed on bleomycin for 4–5 days. Bleomycin treatment causes some stem cells to maintain constant high Ca^{2+} levels, whereas others show reduced oscillation frequency but an increased average GCaMP/RFP intensity (G/R) ratio. These data show that tissue damage by bleomycin triggers stem-cell proliferation, EE production and an increase in cytosolic Ca^{2+}, independently of Piezo. Thirty cells from $n = 4$ (control), $n = 4$ (Bleo+), and $n = 5$ ($Piezo^{KO}$ and Bleo+) independent guts are plotted. **i**, Overexpression of $Piezo^{OE}$ in Esg^+ cells (32 °C) increases the proportion of Dl^+ cells (labelled by *Dl-lacZ*; red) within the Esg^+ population. **j**, *Piezo* overexpression promotes the Dl^+/Esg^+ cell ratio. Ratio between Dl^+ and Esg^+ cells within 10,000-μm^2 regions: $n = 21$ (control) and $n = 22$ ($Piezo^{OE}$) from two independent replicates, are analysed. **k**, **l**, Overexpression of *Piezo* or knockdown of *SERCA* in $Su(H)Gbe^+$ enteroblast cells showed no significant phenotype, suggesting that their effect may be blocked by high Notch activity. Number of midgut areas quantified: $n = 18$ (control), $n = 20$ (*SERCA-i*), $n = 16$ ($Piezo^{OE}$). Data are mean + s.e.m. *P* values are from a two-tailed Student's *t*-test with unequal variance. Scale bars, 50 μm (**a**, **e**, **f**, **k**) and 20 μm (**i**).

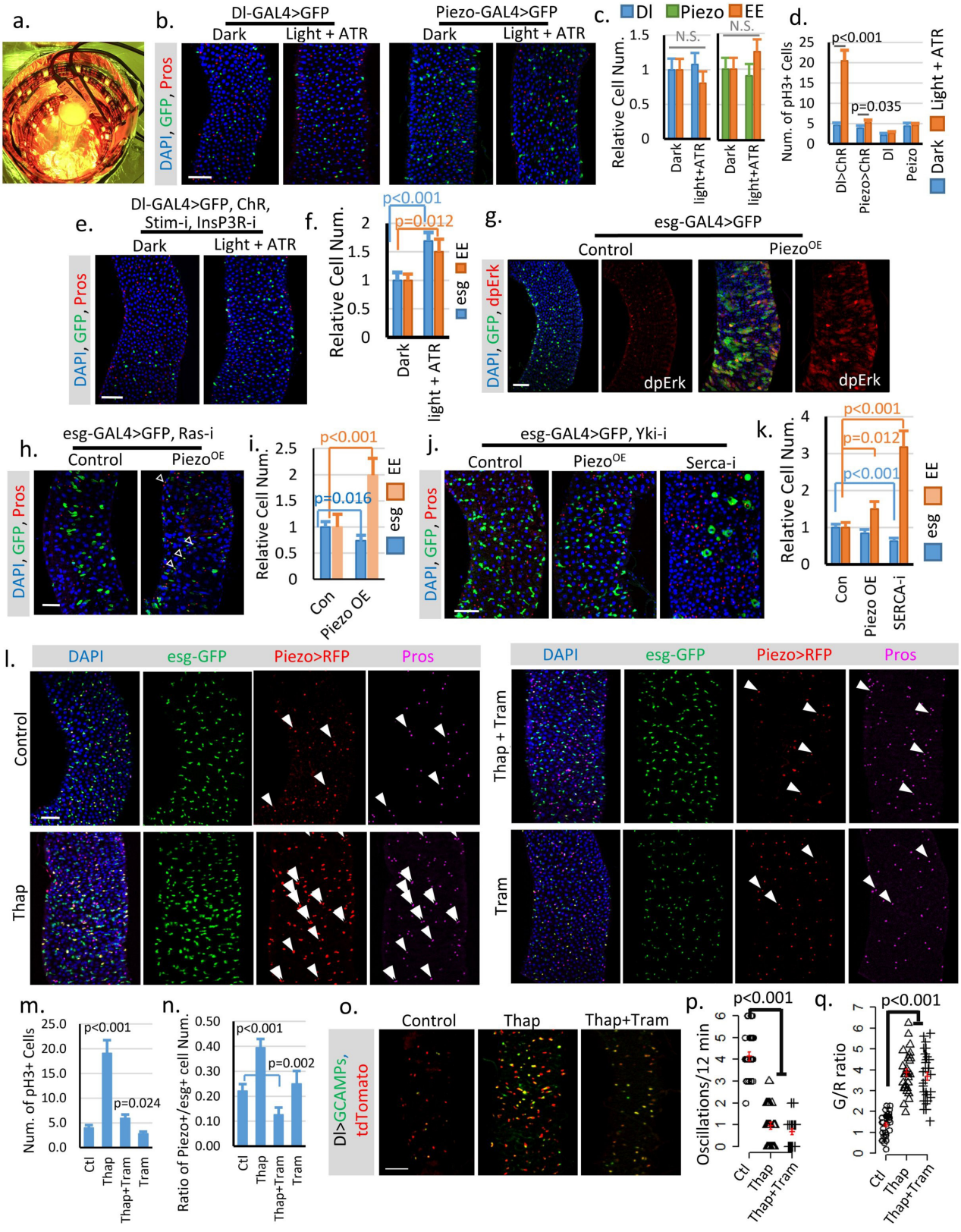

Extended Data Figure 7 | See next page for caption.

Extended Data Figure 7 | Cytosolic Ca^{2+} triggers ISC proliferation and enteroendocrine precursor differentiation into EEs. a, Image of chamber used for optogenetic activation of ChR. **b**, **c**, Flies expressing GFP only in Dl^+ stem cells or $Piezo^+$ enteroendocrine precursor (EE precursor) cells were treated under either dark or light + ATR conditions for 2 weeks, as per the flies expressing ChR. No significant phenotype was induced by the treatment alone. Number of midgut areas quantified: $n = 29$ (Dl, dark), $n = 33$ (Dl, light + ATR), $n = 31$ (Piezo, dark), $n = 34$ (Piezo, light + ATR). Representative results from two independent replicates are shown. **d**, Mitosis quantification of midgut from indicated genotype/condition. Activating ChR in Dl^+ cells significantly promotes stem-cell proliferation. Only a mild increase in mitosis was detected in ChR-active $Piezo^+$ enteroendocrine precursor cells, suggesting that the primary effect of Ca^{2+} in enteroendocrine precursor cells is to promote differentiation. Data are from 30 guts (*Dl>ChR*); 30 guts (*Piezo>ChR*); 29 guts (*Dl*); guts (*Piezo*) from two independent replicates. $pH3^+$ cell number is quantified from the whole midgut. **e**, **f**, Activation of the channelrhodopsin CsChrimson in Dl^+ stem cells with both *Stim* and *InsP3R* knocked down causes a reduced increase in stem cells and EEs compared to wild-type stem cells. Flies were raised at 18 °C and shifted to 25 °C during the experiment. Cell numbers are quantified within a 10,000-μm^2 area from 29 regions (dark) and 31 regions (light + ATR) from two independent replicates. **g**, Overexpression of *Piezo* in Esg^+ cells increases MAPK pathway activity. Phosphorylation of dpErk is significantly increased in *Piezo*-overexpressing cells. Representative images from two independent experiments are shown. **h**, **i**, Knockdown of Ras significantly reduces stem-cell proliferation caused by *Piezo* overexpression, but does not block Piezo-triggered EE differentiation. Flies were kept at 32 °C for 4–5 days before analysis. Esg^+ and EE cell numbers were quantified from $n = 29$ (control) and $n = 30$ ($Piezo^{OE}$) midgut areas from two independent experiments. Arrowheads denote newborn EEs (positive for both Esg and Pros). **j**, **k**, Knockdown of y*orkie* using *yki-i* completely blocks stem-cell proliferation but not the increase of EE cells induced by either *Piezo* overexpression or *SERCA* knockdown. In addition, knockdown of *SERCA* together with *yki* also significantly reduced stem-cell number, suggesting a depletion of stem cells caused by constant EE differentiation. Cell numbers were quantified from 30 midgut areas for each genotype. **l**, Midguts from flies fed on control (5% sucrose), thapsigargin (5% sucrose, 0.5 μM thapsigargin; Thap), thapsigargin + trametinib (5% sucrose, 0.5 μM thapsigargin, 10 μM trametinib; Thap + Tram), and trametinib (5% sucrose, 5 μM trametinib; Tram) for 4 days. Representative images from three independent experiments are shown. The increase of cytosolic Ca^{2+} by thapsigargin promotes stem-cell proliferation, enteroendocrine precursor ($Piezo^+$ cell) production, and EE differentiation. White arrowheads denote newborn EEs (positive for Esg, Piezo and Pros). **m**, Quantification of mitotic cells from $n = 15$ (control), $n = 16$ (Thap), $n = 17$ (Thap + Tram), and $n = 16$ (Tram) midguts. Thapsigargin treatment triggers a significant increase in mitosis, which is largely reduced by the MAPK inhibitor trametinib. **n**, Percentage of $Piezo^+$ cells within the Esg^+ cell population. Number of areas quantified: $n = 29$ (ctl), $n = 31$ (Thap), $n = 32$ (Thap + Tram), $n = 29$ (Tram). **o**, Representative Ca^{2+} images of live midgut from control, thapsigargin-treated, and thapsigargin plus trametinib-treated flies. Similar results were collected from 4 independent guts for each condition. **p**, **q**, Thapsigargin treatment caused a reduction in oscillation frequency but an increase in the average GCaMP/RFP (G/R) ratio. The increase in cytosolic Ca^{2+} by thapsigargin treatment is not affected by MAPK inhibition. Data are from 29 cells from 3 independent guts for each condition. Data are mean + s.e.m. (shown in red). *P* values are from a two-tailed Student's *t*-test with unequal variance. Scale bars, 50 μm.

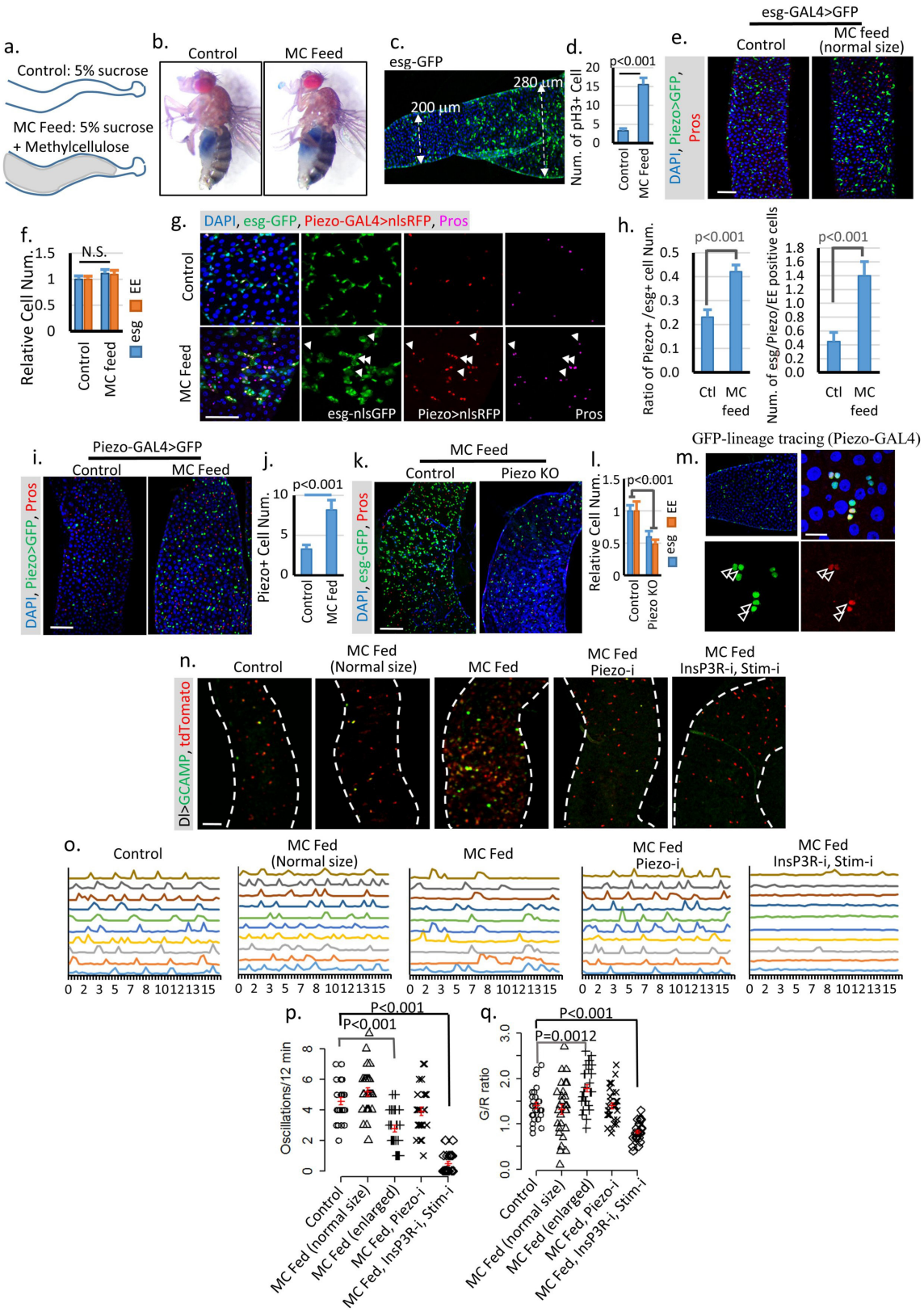

Extended Data Figure 8 | See next page for caption.

Extended Data Figure 8 | Over-feeding triggers stem-cell proliferation and an increase in EEs. a, Schematic illustration of fly midguts from control (5% sucrose) or methylcellulose (5% sucrose plus 10% methylcellulose) fed flies. **b**, 'Smurf' assay of flies fed on both control and methylcellulose food shows no damage to gut integrity. Two independent replicates showed similar results. **c**, **d**, Image of a midgut of a fly fed on methylcellulose food. The cell proliferation phenotype is associated with an increase in midgut diameter but not food content. Data are from 23 midgut areas from 2 independent experiments for each condition. **e**, **f**, Midguts from flies fed methylcellulose with no increase in gut diameter show no change in phenotype compared with control. Data are from 31 regions (control) and 28 regions (MC) from three independent experiments. **g**, **h**, Feeding-induced cell proliferation produces more $Piezo^+$ cells, which differentiate into EEs. White arrowheads denote newborn EEs. Data are from 27 areas from 2 independent experiments for each condition. **i**, **j**, Feeding-induced midgut enlargement triggers a significant increase in the enteroendocrine precursor/$Piezo^+$ cell number. Data are from $n = 30$ (control) and $n = 32$ (MC) midgut areas from 2 independent replicates. **k**, **l**, Feeding-trigged stem-cell proliferation and EE increases are blocked in the *Piezo*-null ($Piezo^{KO}$) mutant. Data are from $n = 27$ (control) and $n = 32$ ($Piezo^{KO}$) midgut areas from 2 independent replicates. **m**, Linage-tracing experiment (using *Piezo-GAL4*) under overfed conditions shows a significant increase in cell number (2–3) in the same cluster compared to tracing result under control conditions, suggesting that either more Piezo cells were created from ISCs or more $Piezo^+$ cells divide to create more progeny. Arrowheads denote cells positive for both GFP and Pros. **n**, Images of live midguts from the following conditions/genotypes: control, methylcellulose fed without midgut diameter increase (normal size), methylcellulose fed with enlarged midgut diameter, methylcellulose fed with *Piezo-i* and enlarged midgut diameter, and methylcellulose fed with *InsP3R-i* + *Stim-i* and enlarged midgut diameter. **o**, Representative traces of Ca^{2+} oscillations in Dl^+ stem cells of flies from indicated treatment/genotypes. Data are from 3 independent experiments for each genotype/condition. **p**, **q**, Ca^{2+} oscillation frequency and GCaMP/RFP intensity ratio of 30 cells from three individual guts for each genotype. Mean ± s.e.m. is displayed in red. Enlarged midgut of fly fed on methylcellulose shows reduced Ca^{2+} oscillation frequency but increased average cytosolic Ca^{2+} level. Methylcellulose alone does not trigger any significant change in Ca^{2+} activity. Knockdown of *Piezo* or of both *Stim* and *InsP3R* blocks this feeding-induced increase in cytosolic Ca^{2+}. Knockdown of *InsP3R* or *Stim* alone has no significant effect on cytosolic Ca^{2+} (data not shown), which is probably due to the reduced expression levels of *Dl-GAL4* compared with *esg-GAL4*. The change in Ca^{2+} activity in enlarged midguts of methylcellulose-fed flies is similar to some cells in the bleomycin-damaged midguts (Extended Data Fig. 6f, g). However, most cells from enlarged midguts of methylcellulose-fed flies still oscillate, which is different from stem cells in bleomycin-treated midguts, in which a large portion of cells maintain a constant high level of Ca^{2+} (Extended Data Fig. 6f, g). Data are mean + s.e.m. *P* values are from a two-tailed Student's *t*-test with unequal variance. Scale bars, 50 μm (**e**, **i**, **k**, **n**), 25 μm (**g**) and 10 μm (**m**).

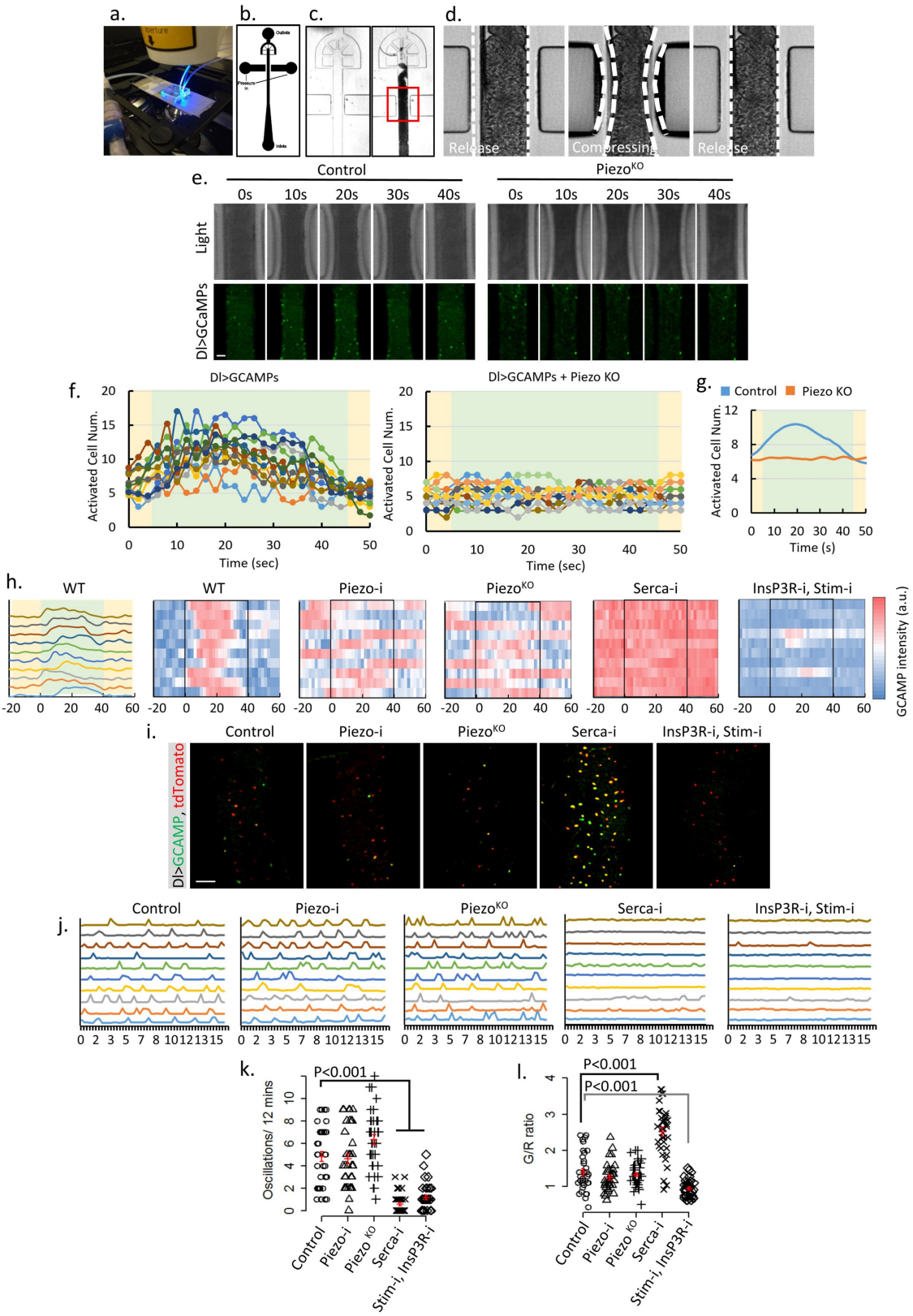

Extended Data Figure 9 | See next page for caption.

Extended Data Figure 9 | Direct mechanical activation of the Piezo channel triggers an increase in cytosolic Ca^{2+} in stem cells. a, Image of the microfluidic chip used for the *ex vivo* mechanical trigger experiment. **b**, **c**, Design of the channels on the microfluidic chip. Compressed air was delivered through the left and right channels and controlled by a manual gauge. Dissected fly midguts were loaded into the main channel (centre) from an inlet at the bottom. **d**, During each compression cycle, the midgut was squeezed to achieve an approximately 30–35% reduction in diameter from both sides. The switching time between compression and relaxation is approximately 1 s. **e**, Representative samples of *ex vivo* mechanical trigger experiment. Time 0 s and 40 s were taken immediately before and after compression. The total compression time is 40 s. Transmission light (top) and GCaMP6s signal (bottom) are shown. Compared to control, the loss of Piezo significantly blocked activation of stem cells by mechanical compression. **f**, Plots of activated cells numbers during one triggering cycle (50 s) for control ($n = 12$) and $Piezo^{KO}$ ($n = 15$) fly midguts. Data were from 4–5 individual midguts. All GCaMP-positive cells (5-fold brighter than the midgut autofluorescence signal) within the field were counted. Periods of compression and relaxation are indicated by green and yellow colours, respectively. **g**, Averaged response curves of multiple compression cycles ($n = 12$ for control and $n = 10$ for $Piezo^{KO}$) from control (blue) and $Piezo^{KO}$ (orange) midguts. **h**, Typical traces of Ca^{2+} activities in wild-type stem cells that respond to the mechanical stimulus. Data are represented in curve plot (first panel) and heat-map plot (second panel). The compression period is from 0 to 40 s (black box). Typical traces of Ca^{2+} activities with indicated genotypes. Stem cells with *Piezo* knockdown or mutant do not respond to the mechanical stimulus. Knockdown of *SERCA* causes a constant high cytosolic Ca^{2+}. Knockdown of both *Stim* and *InsP3R* significantly reduces random Ca^{2+} activities and largely blocks the mechanically triggered Ca^{2+} increase. Data are from three independent experiments for each genotype/condition. **i**, Images of cultured midguts from control, *Piezo-i*, $Piezo^{KO}$, *SERCA-i*, and *InsP3R-i* + *Stim-i* flies. **j**, Typical traces of Ca^{2+} activities in stem cells of indicated genotypes. Data are from three independent guts for each genotype/condition. **k**, **l**, Ca^{2+} oscillation frequency and GCaMP/RFP (G/R) intensity ratio in $n = 35$ cells (control), $n = 35$ cells (*Piezo-i*), $n = 34$ cells ($Piezo^{KO}$), $n = 36$ cells (*SERCA-i*), $n = 33$ cells (*InsP3R-i* + *Stim-i*) from three independent experiment for each condition/genotype. Neither *Piezo-i* nor $Piezo^{KO}$ significantly affect Ca^{2+} activities. Knockdown of *SERCA* induces a constant increase of cytosolic Ca^{2+} in most cells. Knockdown of both *InsP3R* and *Stim* stem cells significantly reduces their Ca^{2+} activities. Our data indicate that mechanical stresses generated during food digestion may activate Piezo and promote EE generation *in vivo*. However, the timescale between our *ex vivo* mechanical activation and *in vivo* cell proliferation and differentiation experiment is very different, especially as the *in vivo* property of Piezo-mediated Ca^{2+} activity in enteroendocrine precursor cells is unknown. According to our observations, only a small percentage (<5%) of $Piezo^{+}$ cells become EEs every day under normal conditions (interpreted from the Piezo and Pros double-positive cell number). Therefore, it is possible that either Piezo is difficult to activate *in vivo* by physiological levels of mechanical stimuli, or long-term cumulative Piezo activation is required to trigger EE differentiation. Mean ± s.e.m. is displayed in red. *P* values are from a two-tailed Student's *t*-test with unequal variance. Scale bars, 50 μm.

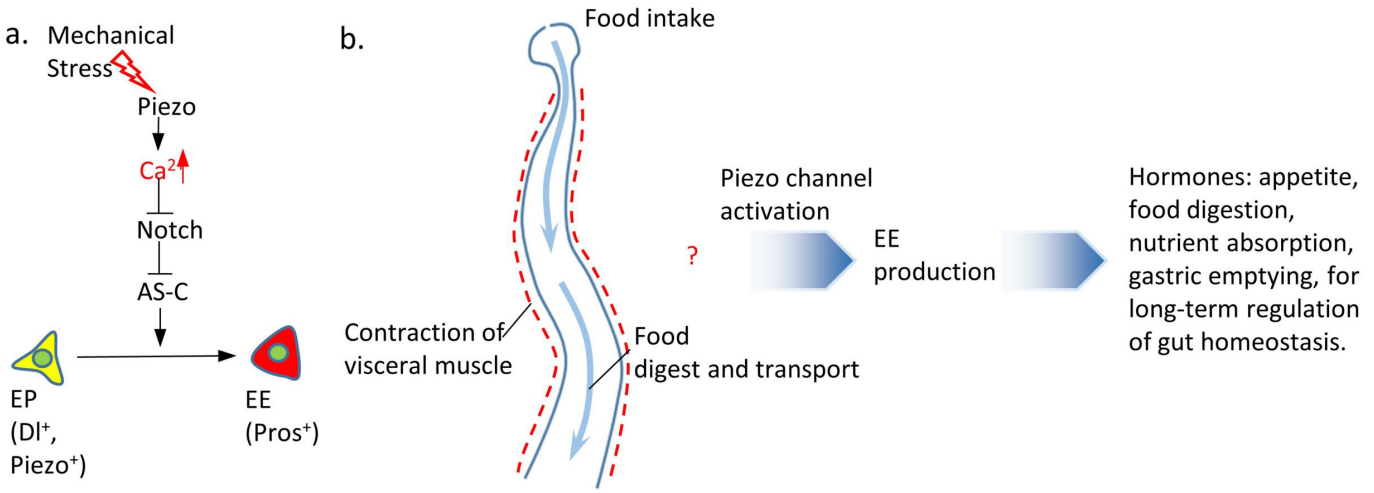

Extended Data Figure 10 | A model of Piezo activation and downstream signalling. a, Under normal conditions, Piezo$^+$ cells, which we refer to as endocrine precursor (EP) cells, are unipotent stem cells that are mitotically quiescent and have a predetermined EE cell fate. In the presence of mechanical stimulation, the Piezo channel is activated and leads to an increase in cytosolic Ca^{2+} in Piezo$^+$ enteroendocrine precursor cells. Ca^{2+} increases in enteroendocrine precursor cells trigger strong cell differentiation into EEs, which is probably mediated by inhibition of Notch activity and consequent increase of AS-C transcription activity. **b**, The presence of food in the intestine triggers increased mechanical stress during food transport and visceral muscle contraction. Our results suggest that mechanical signalling activates the mechanosensitive channel Piezo in quiescent enteroendocrine precursor cells and leads to an increase in cytosolic Ca^{2+} levels, which maintain the basal level EE cell production under physiological conditions and promote fast EE generation under abnormally fed conditions. We hypothesize that, as a key regulator of midgut function, EE cells might secrete hormones to enhance different long-term gastric functions including appetite, digestion, nutrient absorption or gastric emptying.

nature research

Corresponding author(s): Norbert Perrimon, Li He

Life Sciences Reporting Summary

Nature Research wishes to improve the reproducibility of the work that we publish. This form is intended for publication with all accepted life science papers and provides structure for consistency and transparency in reporting. Every life science submission will use this form; some list items might not apply to an individual manuscript, but all fields must be completed for clarity.

For further information on the points included in this form, see Reporting Life Sciences Research. For further information on Nature Research policies, including our data availability policy, see Authors & Referees and the Editorial Policy Checklist.

Please do not complete any field with "not applicable" or n/a. Refer to the help text for what text to use if an item is not relevant to your study.
For final submission: please carefully check your responses for accuracy; you will not be able to make changes later.

Experimental design

1. Sample size

   Describe how sample size was determined.

   Sample sizes were chosen empirically based on the observed effects and listed in the figure legends.

2. Data exclusions

   Describe any data exclusions.

   No Data was excluded.

3. Replication

   Describe the measures taken to verify the reproducibility of the experimental findings.

   All experiments were reliably reproduced.

4. Randomization

   Describe how samples/organisms/participants were allocated into experimental groups.

   No randomization was used as most quantifications were done using automatic cell counting in NIH imageJ.

5. Blinding

   Describe whether the investigators were blinded to group allocation during data collection and/or analysis.

   Experimenter was not blind to fly genotypes.

Note: all in vivo studies must report how sample size was determined and whether blinding and randomization were used.

6. Statistical parameters

   For all figures and tables that use statistical methods, confirm that the following items are present in relevant figure legends (or in the Methods section if additional space is needed).

n/a	Confirmed
☐	☒ The exact sample size (*n*) for each experimental group/condition, given as a discrete number and unit of measurement (animals, litters, cultures, etc.)
☐	☒ A description of how samples were collected, noting whether measurements were taken from distinct samples or whether the same sample was measured repeatedly
☐	☒ A statement indicating how many times each experiment was replicated
☐	☒ The statistical test(s) used and whether they are one- or two-sided *Only common tests should be described solely by name; describe more complex techniques in the Methods section.*
☐	☒ A description of any assumptions or corrections, such as an adjustment for multiple comparisons
☐	☒ Test values indicating whether an effect is present *Provide confidence intervals or give results of significance tests (e.g. P values) as exact values whenever appropriate and with effect sizes noted.*
☐	☒ A clear description of statistics including central tendency (e.g. median, mean) and variation (e.g. standard deviation, interquartile range)
☐	☒ Clearly defined error bars in all relevant figure captions (with explicit mention of central tendency and variation)

See the web collection on statistics for biologists for further resources and guidance.

Software

Policy information about availability of computer code

7. Software

Describe the software used to analyze the data in this study.	NIH imageJ (v. 1.6.0) was used to select and automatically quantification of cell number.

For manuscripts utilizing custom algorithms or software that are central to the paper but not yet described in the published literature, software must be made available to editors and reviewers upon request. We strongly encourage code deposition in a community repository (e.g. GitHub). *Nature Methods* guidance for providing algorithms and software for publication provides further information on this topic.

Materials and reagents

Policy information about availability of materials

8. Materials availability

Indicate whether there are restrictions on availability of unique materials or if these materials are only available for distribution by a third party.	No unique materials were used.

9. Antibodies

Describe the antibodies used and how they were validated for use in the system under study (i.e. assay and species).	The following primary antibodies were used: mouse anti-Prospero (1:50, Developmental Studies Hybridoma Bank, MR1A), rabbit anti-phospho-Histone H3 (Millipore #06–570; 1:1000); mouse anti-HA (Abcam, ab18181), rabbit anti-dpErk1/2 (Cell Signaling #4370; 1:500), mouse anti-Delta (1:50, Developmental Studies Hybridoma Bank, C594.9B), mouse anti-β-galactosidase (1/400, Promega, Z3781), rabbit anti-Tachykinin (1/5000, Veenstra et al.33). Secondary antibodies were goat anti-rabbit and anti-mouse IgGs conjugated to Alexa 555 and Alexa 647 (used at 1:500, Thermofisher, A-21428, A-21244, A-21235, A-21422).

10. Eukaryotic cell lines

a. State the source of each eukaryotic cell line used.	No cell line was used.
b. Describe the method of cell line authentication used.	N.A.
c. Report whether the cell lines were tested for mycoplasma contamination.	N.A.
d. If any of the cell lines used are listed in the database of commonly misidentified cell lines maintained by ICLAC, provide a scientific rationale for their use.	N.A.

Animals and human research participants

Policy information about studies involving animals; when reporting animal research, follow the ARRIVE guidelines

11. Description of research animals

Provide all relevant details on animals and/or animal-derived materials used in the study.	Drosophila melanogaster was the only model organism used in the study. "All the images presented and used for quantification are from the anterior region of adult female fly midgut for consistency. " Stages or ages are stated for specific experiment in the manuscript.

Policy information about studies involving human research participants

12. Description of human research participants

Describe the covariate-relevant population characteristics of the human research participants.	Human participants were not used in the study.